

Lesson 9:

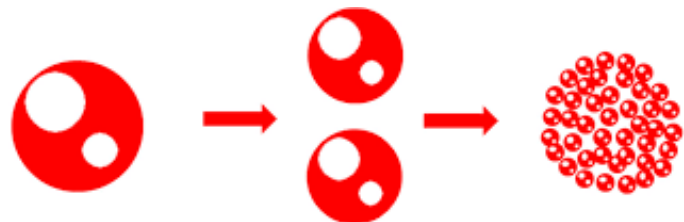
Thermodynamics of Nanostructures

(Size and confinement effects; Surface atoms and surface-volume ratio; Surface energy and surface stress; Effect on lattice parameter; Surface energy and Wulff theorem: Wulff construction and equilibrium shape of nanocrystals; Inverse Wulff construction; Equilibrium Shape of supported nanocrystals: the Wulff-Kaichew theorem; Solid-liquid transition in nanostructures: size-dependent cohesive energy and melting temperature (theoretical models and comparisons to experimental data))

Size Effects on Structure and Morphology of Free or Supported Nanoparticles

Size and Confinement Effects

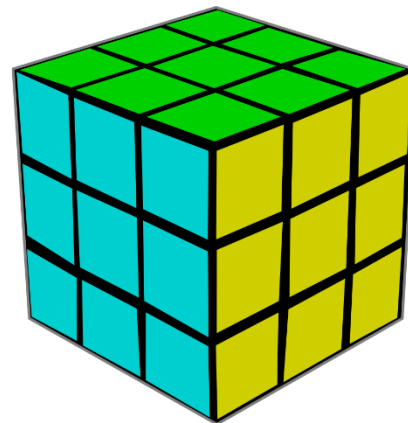
Fraction of Surface Atoms



Increasing surface area

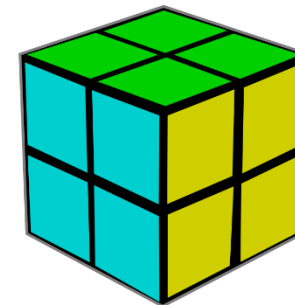
Bulk material

Nanoparticles



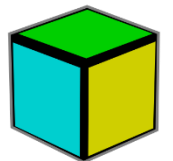
$$\begin{aligned} \text{sides} &= 3 \\ \text{surface} &= 3^2 \times 6 = 54 \\ \text{volume} &= 3^3 = 27 \end{aligned}$$

$$\text{surface/volume} = 2 \text{ m}^{-1}$$



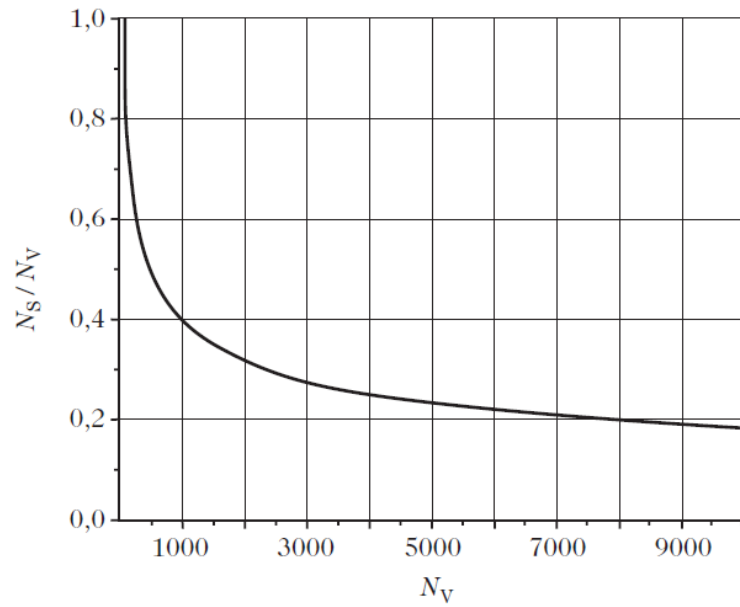
$$\begin{aligned} \text{sides} &= 2 \\ \text{surface} &= 2^2 \times 6 = 24 \\ \text{volume} &= 2^3 = 8 \end{aligned}$$

$$\text{surface/volume} = 3 \text{ m}^{-1}$$



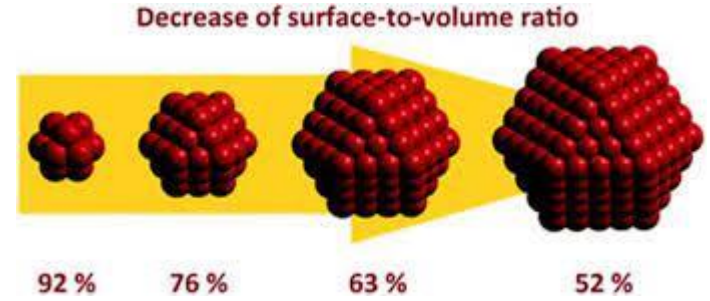
$$\begin{aligned} \text{sides} &= 1 \\ \text{surface} &= 1^2 \times 6 = 6 \\ \text{volume} &= 1^3 = 1 \end{aligned}$$

$$\text{surface/volume} = 6 \text{ m}^{-1}$$



$$\frac{N_s}{N_v} \approx \frac{1}{2R}$$

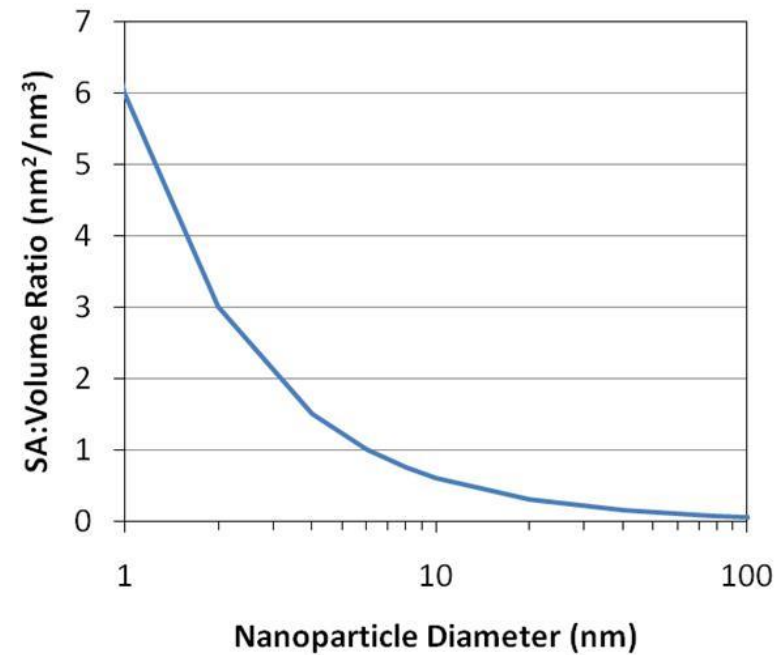
(R in nm)



Surface Area:Volume Ratio

Fig. 1.1. Proportion of surface atoms for a spherical particles comprising N_v atoms with N_s at the surface

Hence, at 5 nm (around 8,000 atoms), this proportion is about 20%, whilst at 2 nm (around 500 atoms), it stands at 50%.



In this graph:

SA = nm²

Vol = nm³

SA:Vol Ratio = nm²/nm³

The ratio increases dramatically when the nanoparticle diameter drops below about 100 nm

$$\frac{N_s}{N_v} \approx \frac{1}{2R}$$

where R is the radius in nm. This empirical law gives a proportion of surface atoms of 100% for a size of 1 nm. Of course, (1.1) is no longer valid for smaller dimensions. We shall see that the fact that a large fraction of the atoms are located at the surface of the object will modify its properties. To tackle this question, we shall need to review certain physical quantities associated with surfaces, namely the specific surface energy and the surface stress.

Reducing the size of a nanocrystal increases the relative importance of the surface or interface between grains. Consequently, the state of the surface or interface also predetermines the properties of the nanomaterial.

The variation of the parameters describing crystal structure can be understood in relation to the nanocrystal surface using either thermodynamic or microscopic approaches.

The state of the surface or interface of a nanocrystal can affect the crystal structure parameters. However, it is still difficult to predict this effect or estimate its importance.

The thermodynamics of nanosystems differs significantly from the thermodynamics of macroscopic systems, because a certain number of variables such as the energy, entropy, etc., are only extensive in the thermodynamic limit, i.e., when the number of particles making up the system tends to infinity. Likewise, the equivalence of the Gibbs ensembles (microcanonical, canonical, and grand canonical) is only valid in this same limit. We shall see later (see

In the framework of statistical thermodynamics, Gibbs defined three so-called ensembles, corresponding a priori to different physical situations [1]. However, these ensembles provide completely equivalent descriptions of macroscopic systems in the thermodynamic limit. Let us recall their main features:

- Microcanonical Ensemble. The system is assumed isolated so that its energy is constant. All the microscopic states corresponding to a given macroscopic state are equiprobable.
- Canonical Ensemble. The system has fixed composition, but it can exchange energy with a thermostat at temperature T . The probability of occupation of an energy state E is proportional to the Boltzmann factor $\exp(-E/k_{\text{B}}T)$.
- Grand Canonical Ensemble. The system can exchange energy with a thermostat of temperature T and components with a reservoir of particles having chemical potential μ . The occupation probability of an N -particle state with energy E is proportional to $\exp[-(E - \mu N)/k_{\text{B}}T]$.

Thermodynamics of Very Small Systems

Consider a simple thermodynamic system with volume V and containing N particles. This system is characterised by a function called the density of states, given in classical mechanics by an integral over the phase space, viz.,

$$\Omega(E, V, N) = \frac{d}{dE} \int_{H(\mathbf{q}, \mathbf{p}) \leq E, \mathbf{q} \in V} d\mathbf{q}d\mathbf{p} , \quad (3.11)$$

where \mathbf{q} stands for all position coordinates, \mathbf{p} stands for the generalised momenta, and E is the total energy of the system. In quantum mechanics, the density of states is defined rather differently, but raises no particular difficulties in this context. We consider the following Gibbs ensembles:

- *Microcanonical Ensemble.* Variables (E, V, N) . Entropy and temperature given by

$$S_\mu(E, V, N) = k_B \ln [\Omega(E)] , \quad (3.12)$$

$$T_\mu(E, V, N) = \left(\frac{\partial S}{\partial E} \right)^{-1} . \quad (3.13)$$

- *Canonical Ensemble.* Variables (T, V, N) . Setting $\beta = 1/k_B T$, the partition function $Z(\beta, V, N)$ is defined by

$$Z(\beta, V, N) = \int \Omega(E, V, N) e^{-\beta E} dE . \quad (3.14)$$

The entropy S and internal energy U are given by

$$U(\beta, V, N) = \frac{\int E \Omega(E, V, N) e^{-\beta E} dE}{Z(\beta, V, N)} , \quad (3.15)$$

$$S(\beta, V, N) = \frac{U(\beta, V, N)}{T} + k_B \ln [Z(\beta, V, N)] . \quad (3.16)$$

- *Grand Canonical Ensemble.* Particles have variable size N . Since we wish to obtain the behaviour of a cluster of given size, we shall not consider this ensemble here.

In the thermodynamic limit, i.e., when $N \rightarrow \infty$ with $U/N \rightarrow u$ and $V/N \rightarrow v$ (u and v finite), the microcanonical and canonical ensembles lead to the same predictions. This is what is meant by the equivalence of the ensembles. Moreover, there is a function $s(u, v)$ such that, as $N \rightarrow \infty$, the entropy per molecule $S/N \rightarrow s$. This is why the entropy is treated as an extensive function. However, for finite N , neither of these two properties is satisfied. The

In small clusters, the thermodynamic properties can vary enormously from one size to another, and there is really no place for extensivity here.

Even if size effects such as structural changes or the influence of the surface can be quantitatively important, they do not lead to a qualitative change in the thermodynamic properties of single phase systems. On the other hand, phase transitions can be considerably altered:

- reduction of the transition temperature,
- reduction of the latent heat,
- broadening of the temperature range over which phases can coexist.

Moreover, phase transitions are a typically polyatomic effect. To characterise a phase, a certain minimum number of constituents is required. It makes no sense, for example, to ask whether a diatomic molecule is liquid or solid. But then, is there a size or size range for which phase transitions disappear?

Basic Elements of Thermodynamics of Surfaces

from A. Zangwill, *Physics at Surfaces*, Cambridge university Press

Bulk Thermodynamics: A Short Reminder

One-component system, in equilibrium, are described completely by the **internal energy** U

$$U = U(S, V, N)$$

where S is the **entropy**, V the **volume**, and N the **number of moles**.

The infinitesimal variation of U is thereby

$$dU = \left(\frac{\partial U}{\partial S} \right)_{V,N} dS + \left(\frac{\partial U}{\partial V} \right)_{S,N} dV + \left(\frac{\partial U}{\partial N} \right)_{S,V} dN$$

which becomes:

$$dU = TdS - pdV + \mu dN \qquad U = TS - pV + \mu N$$

where T is the **absolute temperature**, p the **pressure**, and μ the **chemical potential**.

By combining the above equations one arrives at the **Gibbs-Duhem** equation among the intensive variables

$$SdT - Vdp + Nd\mu = 0$$

Bulk + Surface Thermodynamics

When a surface of area A is created, via a cleavage process, the total internal energy of the system must increase by an amount proportional to A , since this process is not spontaneous.

$$U = TS - pV + \mu N + \boxed{\gamma A}$$

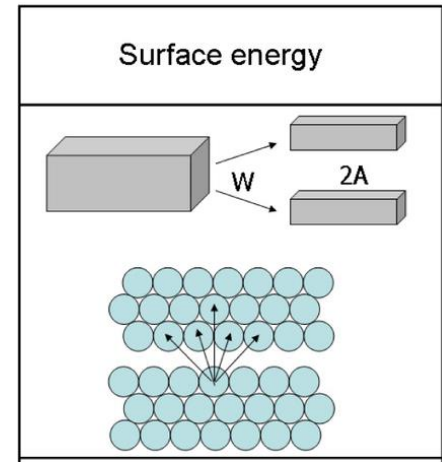
where γ is the constant of proportionality which is called **surface tension**.

Specific Surface Energy and Surface Stress

The specific surface energy γ (J/m²) can be represented as the energy produced by cleaving a crystal divided by the surface area thereby created. More generally, the specific surface energy can be defined as follows. In order to increase the surface area of an object by an amount dA , e.g., by changing the shape of the object, the work required to do this will be

$$\boxed{dW = \gamma dA}. \quad (1.2)$$

γ is the specific surface energy. In this case, the area of the object has increased by displacing atoms from the bulk to the surface. However, one could also increase the area by stretching it, i.e., keeping the number of surface atoms constant. The work required to do this will then be



$$dW = g_{ij}dA, \quad (1.3)$$

where g_{ij} is the surface stress in J/m^2 . This is a tensorial quantity because it depends on the crystallographic axes. The surface stress is related to the elastic stresses resulting from deformation of the surface (strain). It is related to the specific surface energy by

$$g_{ij} = \delta_{ij}\gamma + \frac{\partial\gamma}{\partial u_{ij}}, \quad (1.4)$$

where u_{ij} is the strain tensor and δ_{ij} the Kronecker symbol. Note that for a liquid there is no strain tensor and $g_{ij} = \gamma$. Indeed, if one tries to increase the surface area of a liquid, the bulk atoms will move to the surface to keep the density constant. The surface stress reduces to the specific surface energy.

$\sigma = g$
 $u = \epsilon$
 on the basis of
 used text

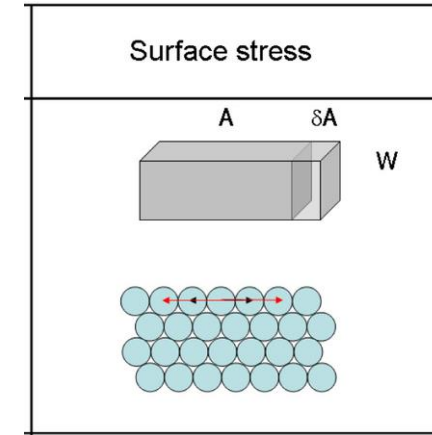
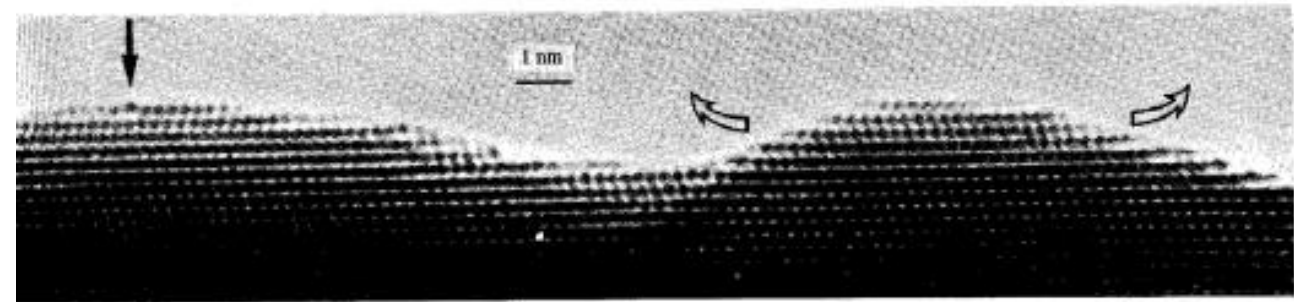


Fig. 1.3. A Au(111) surface buckled under surface stresses. Vertical arrow marks a surface dislocation (Marks, Heine & Smith, 1984).



Now, consider the effect of infinitesimal variations in the area of the system, e.g. by **stretching**. Assuming the **linear elastic theory** holds, one gets

$$dU = \left(\frac{\partial U}{\partial S} \right)_{V,N,A} dS + \left(\frac{\partial U}{\partial V} \right)_{S,N,A} dV + \left(\frac{\partial U}{\partial N} \right)_{S,V,A} dN + A \sum_{i,j} \left(\frac{\partial U}{\partial \varepsilon_{ij}} \right)_{S,V,N} d\varepsilon_{ij}$$

$$dU = TdS - pdV + \mu dN + A \sum_{ij} \sigma_{ij} d\varepsilon_{ij}$$

Where σ_{ij} and ε_{ij} are the components of the **surface stress** and **surface strain** tensors, respectively.

Warning: Be aware of the dimensions of σ_{ij} and ε_{ij} $dA/A = \sum_{i,j} d\varepsilon_{ij} \delta_{ij}$

$$\sigma = \gamma$$

$$u = \varepsilon$$

on the basis of used text

Gibbs-Duhem equation

$$Ad\gamma + SdT - Vdp + Nd\mu + A \sum_{i,j} (\gamma \delta_{ij} - \sigma_{ij}) d\varepsilon_{ij} = 0$$

Surface energy

$$\gamma = E_{coh} (Z_s / Z) N_s$$

where E_{coh} is the bulk cohesive energy, (Z_s/Z) the fractional number of bonds broken (per surface atom), and N_s the surface areal density.

Using typical values:

$E_{coh} \approx 3\text{eV}$, $(Z_s/Z) \approx 0.25$, $N_s \approx 10^{15}$ atoms/cm² we get $\gamma \approx 1,200$ erg/cm²

(from an atomic point of view, E_{coh} = cohesive energy)

Fig. 1.4. Surface tension of the elements in the liquid phase (Schmit, 1974).

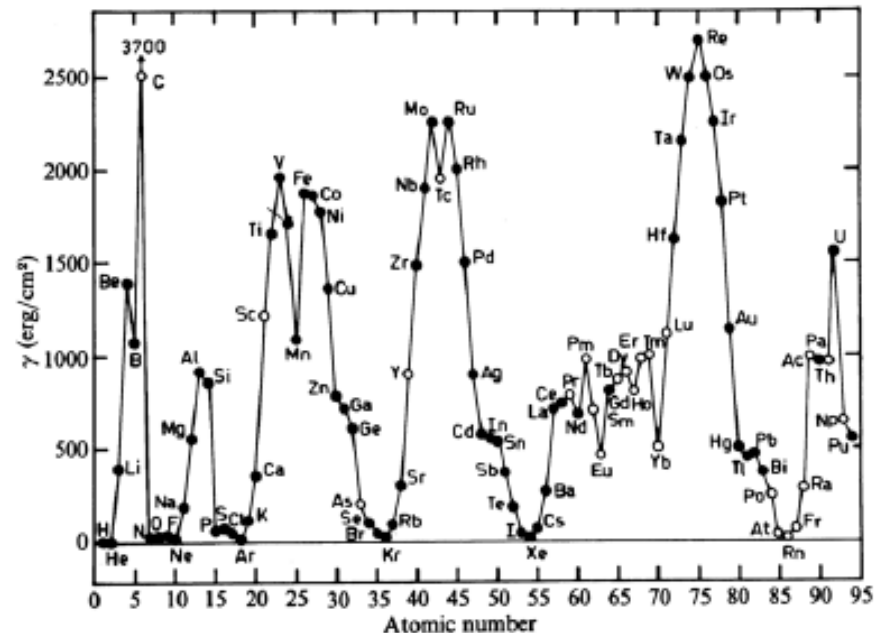


Table 1. Surface tension calculated from equation (3), σ_{calc} , compared with experimental values, σ_{exp} , of Egry et al (1994).

Metal	T/K	$\sigma_{\text{exp}}/\text{N m}^{-1}$	$\sigma_{\text{calc}}/\text{N m}^{-1}$	Deviation/%
Copper	1223	1.333	1.330	-0.23
	1273	1.322	1.321	-0.08
	1323	1.311	1.311	0.00
	1373	1.300	1.301	0.08
	1423	1.289	1.291	0.16
	1473	1.278	1.282	0.31
	1523	1.267	1.272	0.40
	1573	1.256	1.262	0.48
	1623	1.245	1.253	0.64
	1673	1.234	1.243	0.73
	1723	1.223	1.233	0.82
Gold	1323	1.122	1.123	0.09
	1373	1.118	1.118	0.00
	1423	1.113	1.113	0.00
	1473	1.109	1.108	-0.09
	1523	1.104	1.103	-0.09
	1573	1.100	1.099	-0.09
	1623	1.095	1.094	-0.09
	1673	1.091	1.089	-0.18
	1723	1.086	1.084	-0.18
	1773	1.082	1.079	-0.28
	1823	1.077	1.074	-0.28
1873	1.073	1.070	-0.28	
Silver	1193	0.9154	0.9160	0.07
	1236	0.9076	0.9079	0.03
	1279	0.8999	0.8999	0.00
	1322	0.8922	0.8918	-0.05
	1365	0.8844	0.8838	-0.07
	1408	0.8767	0.8757	-0.11
	1451	0.8689	0.8677	-0.14
	1494	0.8612	0.8596	-0.19
	1537	0.8535	0.8516	-0.22
	1580	0.8457	0.8436	-0.25
	1623	0.8380	0.8355	-0.30

Applied Surface Science 257 (2011) 6372–6379



Contents lists available at ScienceDirect

Applied Surface Science

journal homepage: www.elsevier.com/locate/apsusc



Surface energies of metals in both liquid and solid states

Fathi Aqra*, Ahmed Ayyad

Department of Chemistry, Faculty of Science and Technology, Hebron University, P.O. Box 40, Hebron, West Bank, Palestine

$$\gamma(T) = \gamma(T_m) + \frac{d\gamma}{dT} (T - T_m) (\text{mJ m}^{-2})$$

Table 2

Calculated and reported data of metals (s and p blocks), and parameters needed for calculations.

Metal	T_m (K)	T_b (K)	γ_m (mJ m ⁻²)		γ_{SV} (mJ m ⁻²)		α_m (K ⁻¹)	α_b (K ⁻¹)	$-\text{d}\gamma/\text{d}T$ (mJ m ⁻² K ⁻¹)		$-\text{d}\gamma/\text{d}T$ (mJ m ⁻² K ⁻¹)	H_s (mJ m ⁻²)		c_m (ms ⁻¹)		$-\text{d}c/\text{d}T$ (ms ⁻¹ K ⁻¹)	
			Cal.	Rep.	Cal.	Rep.	$\times 10^4$	$\times 10^4$	Cal. I	Cal. II	Reported	Cal. I	Cal II	Cal	Rep	Cal	Rep
Li	453	1615	441	404	618	525	3.0	0.86	0.11	0.16	0.15, 0.16	491	513	5276	5128	1.3	1.7
Na	371	1156	190	197	266	260	3.7	1.20	0.07	0.09	0.09, 0.10	216	223	2634	2699	0.96	1.26
K	336	1032	101	110	141	130	4.1	1.34	0.04	0.06	0.07, 0.08	114	121	1925	1966	0.79	0.84
Rb	312	961	87	85	122	110	4.4	1.44	0.04	0.05	0.06, 0.07	99	102	1256	1251	0.55	0.49
Cs	301	944	68	70	95	95	4.6	1.47	0.03	0.04	0.05, 0.06	77	80	986	983	0.44	0.49
Be	1560	2742	1601	1350	2245	2700	0.89	0.50	0.39	0.28	0.24, 0.29	2209	2038	8635	8825	2.09	1.49
Mg	923	1363	356	557	499	760	1.5	1.02	0.23	0.12	0.14, 0.15, 0.26	568	466	4067	4065	2.65	1.72
Ca	1115	1757	284	337	398	490	1.2	0.79	0.13	0.05	0.09, 0.10, 0.11	429	339	3463	3533	1.54	0.75
Sr	1050	1655	223	286	312	410	1.3	0.84	0.10	0.06	0.08	328	286	2278	2316	1.08	0.83
Ba	1000	2170	225	226	315	370	1.4	0.64	0.06	0.05	0.07	285	275	1772	1751	0.43	0.57
Al	933	2792	985	1070	1381	1160	1.5	0.49	0.15	0.20	0.15, 0.16, 0.19	1125	1171	3855	3944	0.59	0.48
Ga	303	2477	713	708	1000	-	4.6	0.56	0.09	0.19	0.09	740	770	1374	1398	0.18	0.26
In	430	2345	569	560	798	-	3.2	0.59	0.09	0.15	0.10	608	633	1268	1297	0.19	0.29
Tl	577	1746	396	459	555	-	2.4	0.79	0.10	0.12	0.09, 0.11	454	465	1103	1127	0.27	0.23
Si	1687	3538	876	875	1228	1230	0.82	0.39	0.13	0.13	0.22, 0.13, 0.20, 0.28	1095	1095	5091	4922	0.79	0.89
Ge	1211	3106	571	580	800	1060	1.1	0.44	0.08	0.10	0.08	668	692	2690	2693	0.40	0.28
Sn	505	2875	689	640	966	-	2.7	0.48	0.08	0.15	0.09, 0.13, 0.15	729	764	1356	1383	0.16	0.28
Pb	600	2022	388	457	544	-	2.3	0.68	0.08	0.11	0.10, 0.11, 0.12	436	454	1116	1103	0.22	0.28
Sb	904	1860	388	385	544	-	1.5	0.74	0.11	0.10	0.11	487	478	1792	1848	0.53	0.23
Bi	545	1837	383	382	537	-	2.5	0.75	0.08	0.12	0.06, 0.07, 0.08	426	448	1059	1082	0.24	0.21

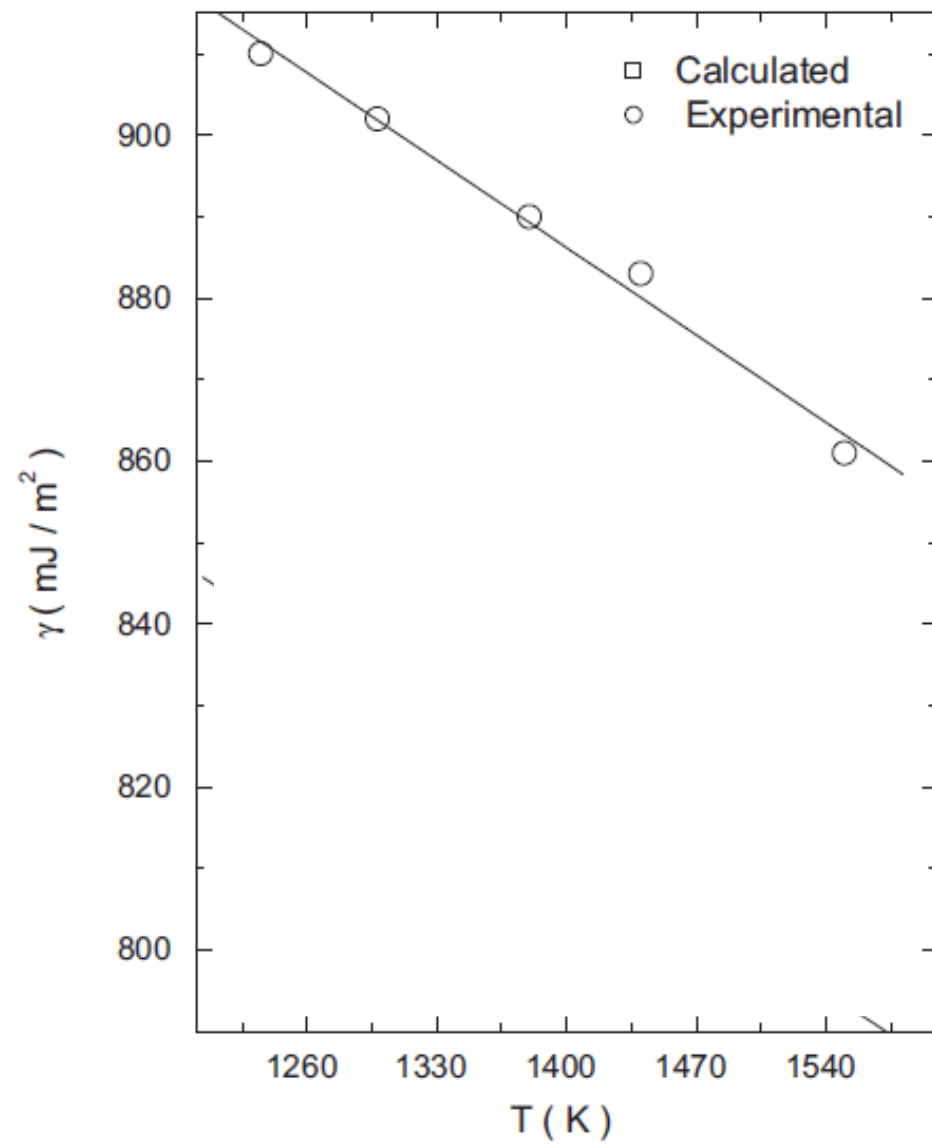


Fig. 2. Calculated (squares) and reported experimental [86] (circles) surface tension of pure liquid silver, in the range 1235–1550 K.

Anisotropy of γ

The surface tension of a planar solid depend on the crystallographic orientation.

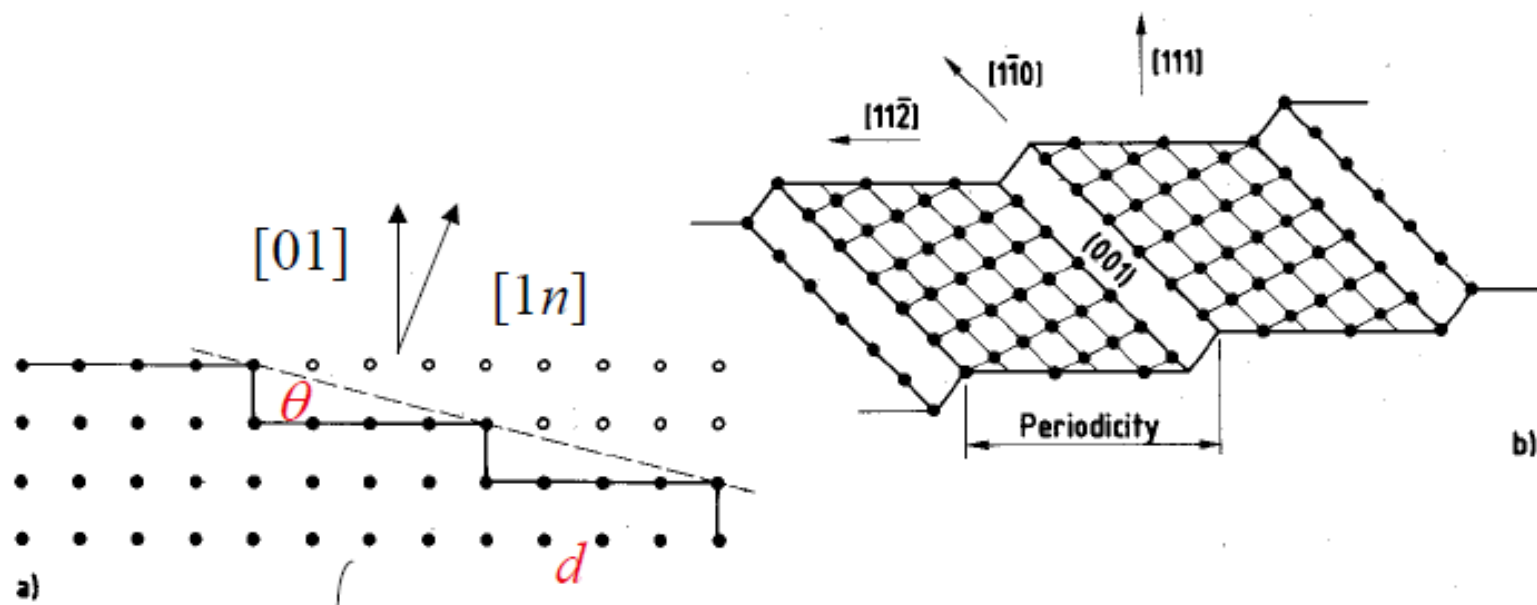


Fig. 3.7a, b. Vicinal surface, a section, b (557) or $[6(111) \times (001)]$ FCC

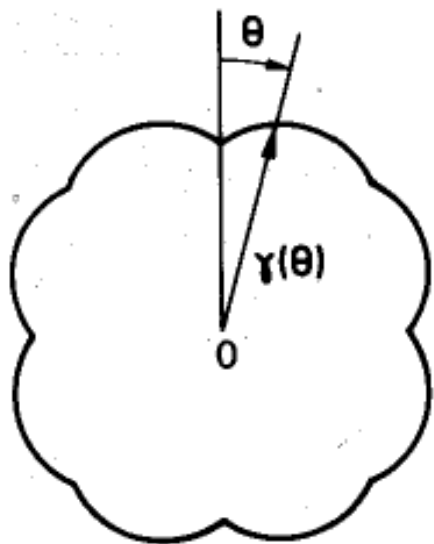
Vicinal surface: A surface slightly **misaligned** from a specific direction. A **vicinal surface** shows a periodic succession of **terraces** and **steps**. If β is the energy per unit length of a step we get

$$\gamma(\mathbf{n}) = \gamma(\mathbf{n}_0) + \frac{\beta|\theta|}{d}$$

where \mathbf{n}_0 defines a close-packed surface, θ is the angle between \mathbf{n} and \mathbf{n}_0 , d is the interplanar distance along \mathbf{n}_0 .

The **anisotropy** of the **surface tension** is represented via the **γ -plot**:

Draw a vector from **O** in the direction **n** (defined by its polar and azimuthal angles θ and ϕ) with a length equal to the surface tension, $\gamma(\mathbf{n})$, for a surface plane perpendicular to **n**.



Example of
a **γ -plot**

The **asphericity** of the **γ -plot** reflects the **anisotropy** of γ which has **minima** in the directions **n₀** corresponding to **close-packed surfaces**.

Fig. 2.2. An example of a γ -plot

Notice that

$|\theta|/d$

is the **density of steps**

$d\gamma/d\theta$ has **discontinuities** at $\theta=0$ and the **γ -plot** shows **cusps** in directions typical of the **most close-packed surfaces**.

$$\gamma(\mathbf{n}) = \gamma(\mathbf{n}_0) + \frac{\beta|\theta|}{d} \quad \Delta\left(\frac{d\gamma}{d\theta}\right)_{\theta=0} = 2(\beta/d)$$

For θ large, the density of steps increases and one has to include the **energy of interaction between steps**.

Landau (1965) showed that $\chi(\theta)$ has a **cusp at every angle of a rational Miller index**. The sharpness of the cusp is a rapidly decreasing function of index:

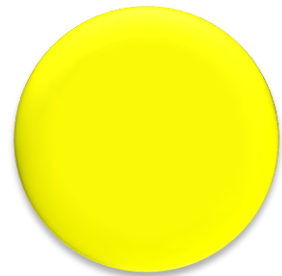
$$\left(\frac{d\gamma}{d\theta} \right) \approx \frac{1}{n^4}$$

Effect on the Lattice Parameter

Let us now consider the effects of the increase in the surface-to-volume ratio as the object size decreases. To do this, we consider first the very simple case of a liquid sphere of diameter $2R$. Due to the curvature of the surface, a pressure is generated toward the inside of the sphere. The excess pressure ΔP inside the sphere, in the purely hydrostatic case, is given by the Laplace equation

$$\Delta P dV = \gamma dA , \quad (1.5)$$

where dV is the volume change corresponding to a change dA in the area of the droplet. In the case of a sphere, (1.5) takes the form


$$\Delta P = \frac{2\gamma}{R} . \quad (1.6)$$

For a spherical solid, the specific surface energy must be replaced by the surface stress tensor g_{ij} . To simplify the problem, consider the case of a solid with simple cubic structure. In this case, γ is isotropic and we have

$$g = \gamma + A \frac{d\gamma}{dA} . \quad (1.7)$$

Moreover, we may recall the definition of the compressibility, viz.,

$$\chi = -\frac{\Delta V}{v\Delta P} , \quad (1.8)$$

where v is the atomic volume of the solid, which can also be defined as a^3 , where a is the lattice parameter. Combining (1.5) and (1.8), We obtain the relative variation of the lattice parameter:

$$\frac{\Delta a}{a} = -\frac{2}{3}\chi \frac{g}{R} .$$

We thus find that there is a contraction of the crystal lattice due to the pressure exerted toward the interior of the particle. This contraction is proportional to the surface stress and inversely proportional to the particle size.

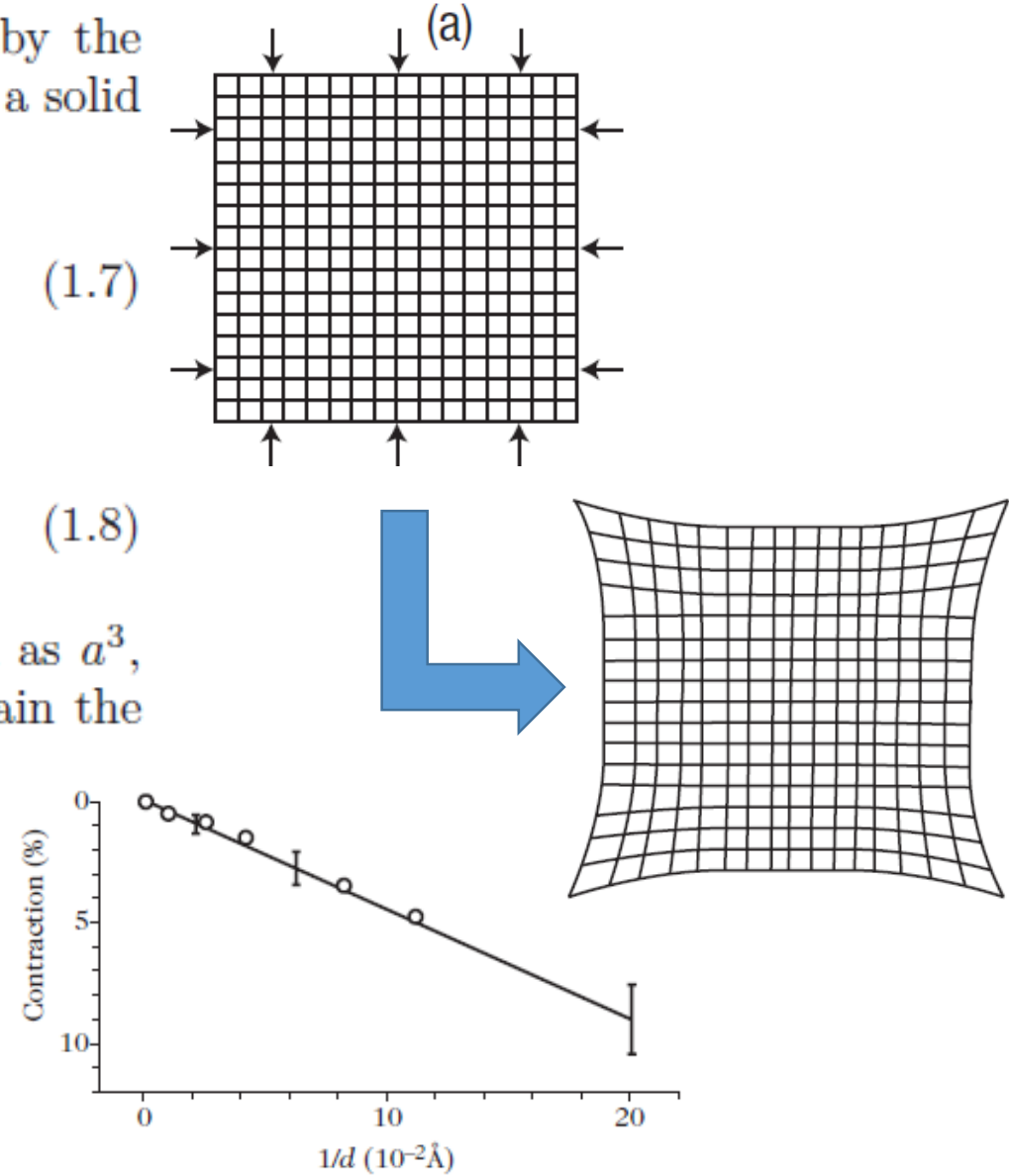


Fig. 1.2. Contraction of the lattice parameter of copper clusters as a function of the reciprocal of their diameter. *Circles* correspond to measurements of electron energy loss near an ionisation threshold (SEELFS). Taken from De Crescenzi et al. [1]. The *straight line* shows measurements of X-ray absorption (EXAFS). Taken from Apai et al. [2]

From Semi-infinite Crystals to nanostructures

Limited by a plane S with its normal at $\theta=0$

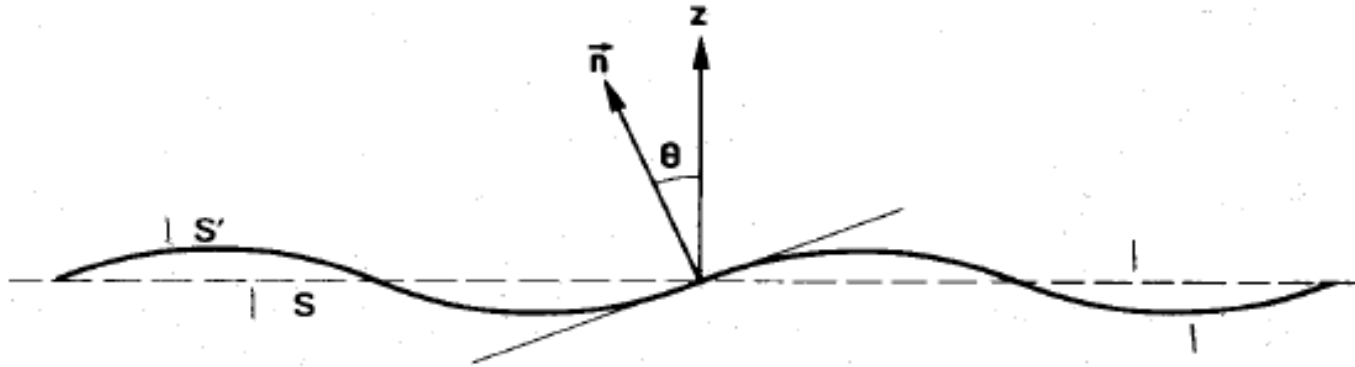


Fig. 2.3. Small polar buckling of a planar surface

Now let us study its **stability** relative to a **small polar buckling** preserving the average orientation.

The free energy of the buckled S' surface is

$$F_{S'} = \int_{S'} \gamma(\theta) dS' = \int_{S'} \gamma(\theta) \frac{dS}{\cos \theta}$$

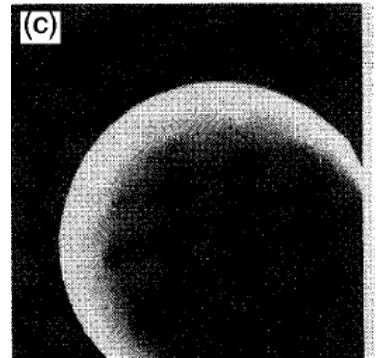
An expansion up to second order in θ gives:

$$F_{s'} = \gamma(0)S + \int_S \theta \left[\frac{d\gamma}{d\theta} \right]_{\theta=0} dS + \frac{1}{2} \int_S \theta^2 \left[\frac{d^2\gamma}{d\theta^2} + \gamma(\theta) \right]_{\theta=0} dS$$

The second term vanishes for symmetry reasons and the **energy involved in the deformation is thus the last term**

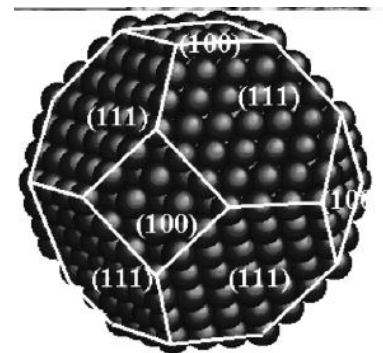
$$\gamma(0) + (d^2\gamma/d\theta^2)_{\theta=0} < 0$$

The surface is **stable** (or **metastable**)



$$\gamma(0) + (d^2\gamma/d\theta^2)_{\theta=0} > 0$$

The surface is **unstable** and will minimize its energy by **developing facets**

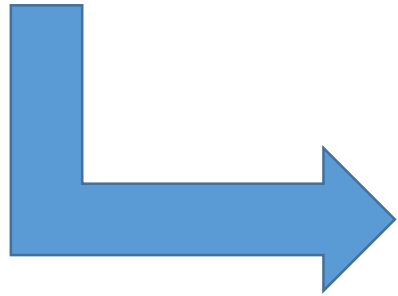


Finite Crystal or Nanostructure

Limited by a surface S .

The equilibrium shape must minimize the excess surface free energy while preserving the volume:

$$F_s = \iint_S \gamma(\mathbf{n}) dS$$



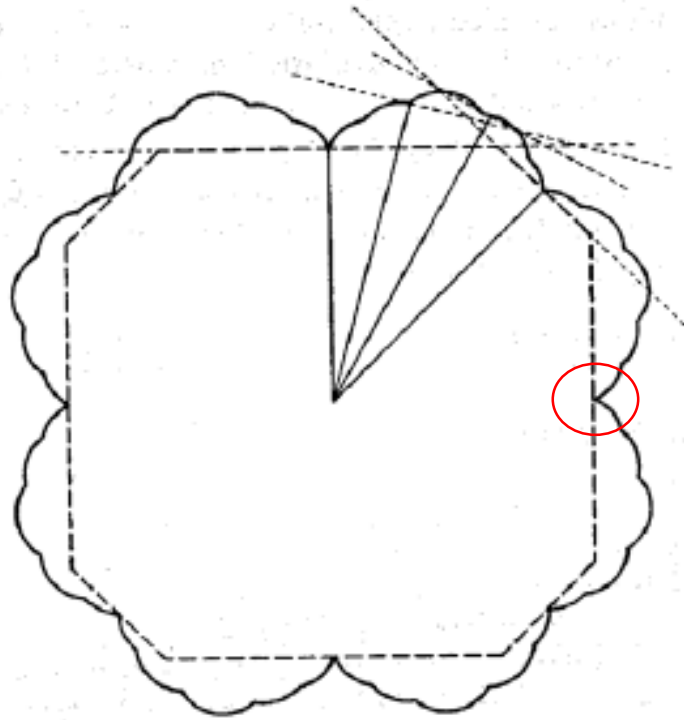
Equilibrium (Thermodynamic) Shape of a Nanocrystal: The Wulff Construction (T=0 K)

Construction of the Wulff equilibrium shape from a γ plot

The variational geometric problem was solved by **Wulff** (1901).

- Draw a radius vector intersecting the polar plot at one point and making a fixed angle with the horizontal
- Construct the plane perpendicular to the vector at the point of intersection.
- Repeat this procedure for all angles.

Fig. 1.6. Polar plot of the surface tension at $T = 0$ (solid curve) and the Wulff construction of the equilibrium crystal shape (dashed curve) (Herring, 1951b).



Minimi Assoluti

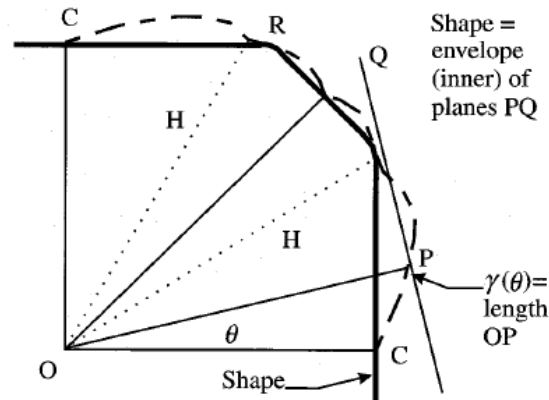


Figure 1.5. A 2D cut of a γ -plot, where the length OP is proportional to $\gamma(\theta)$, showing the cusps C and H , and the construction of the planes PQ perpendicular to OP through the points P . This particular plot leads to the existence of facets and rounded (rough) regions at R . See text for discussion

under conditions of thermodynamic equilibrium, the shape of a crystal is unique. This last result was first obtained by Wulff over a century ago [12]. The solution to this problem consists in minimising the total surface energy E_s . For a liquid the result is immediate: one obtains a sphere. For a crystal, the specific surface energy γ depends on the orientation of the crystal face. One must therefore minimise

$$E_s = \sum_i \gamma_i A_i, \quad (1.10)$$

where the index i represents the different facets with areas A_i and specific surface energy γ_i . Wulff showed that the minimal energy is obtained for a polyhedron in which the central distances h_i to the faces are proportional to their surface energies γ_i . This is the well-known Wulff theorem:

$$\frac{\gamma_i}{h_i} = \text{constant}. \quad (1.11)$$

$$\frac{\gamma_{hkl}}{R_{hkl}} = \text{const.}$$

orientation (γ -graph). Consider a projection of the γ -graph along an axis of symmetry of the crystal, as shown in Fig. 1.4. Starting from the center of symmetry O , draw the radial vectors out to each point of the γ -graph and then draw straight lines normal to the radial vectors at these points. The inner envelope obtained from the set of all these normals represents the projection of the equilibrium shape of the crystal along the chosen crystal axis (a hexagon in the case illustrated). It is clear from the figure that the facets of the equilibrium shape correspond to the cusps of the γ -graph at the minima of the surface energy. When the temperature of the crystal comes close to the melting temperature, the cusps will be less and less deep (the anisotropy of the surface energy decreases) and the equilibrium shape tends to spherical.

At 0 K, the equilibrium shape contains only a few different faces with the lowest surface energies. For metals with face centered cubic (fcc) structure, the equilibrium shape is a truncated octahedron exposing the faces (111) and (100) (see Fig. 1.5). For a metal with body centered cubic (bcc) structure, the shape is a dodecahedron. For ionic crystals which have a high degree of surface energy anisotropy, a single face shows up and the equilibrium shape of crystals like NaCl or MgO is a cube.

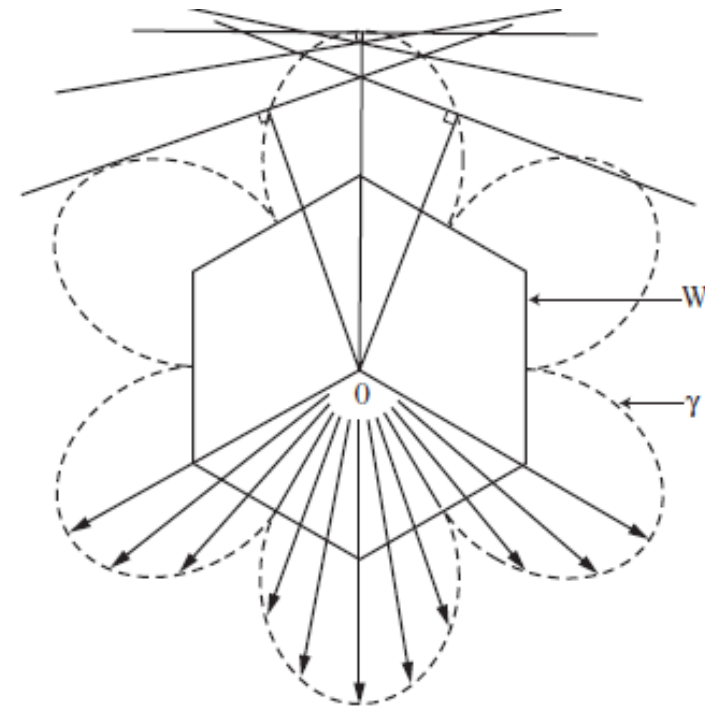


Fig. 1.4. Wulff construction of the equilibrium shape of a crystal from the γ -graph (*dashed curve*). O is the center of the crystal. The hexagon represents a projection of the equilibrium shape of the crystal (Wulff polyhedron). From [11]



Fig. 1.5. Morphology of nanoparticles. (a) Truncated octahedron with 201 atoms. (b) Cubo-octahedron with 147 atoms. (c) Icosahedron with 147 atoms. (d) Truncated decahedron with 146 atoms

Table 1.1. Magic numbers for different clusters: icosahedron, cubo-octahedron, truncated (Marks) decahedron, and truncated octahedron (Wulff polyhedron for an fcc crystal)

Icosahedron,								
cubo-octahedron	13	55	147	309	561	923	1415	2057
Marks decahedron	75	100	146	192	238	247	268	318
Truncated octahedron	38	116	201	225	314	405	807	1289

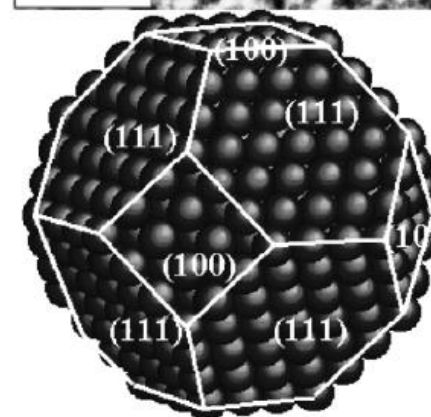
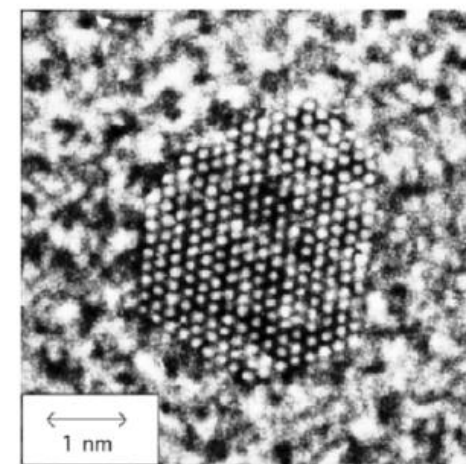
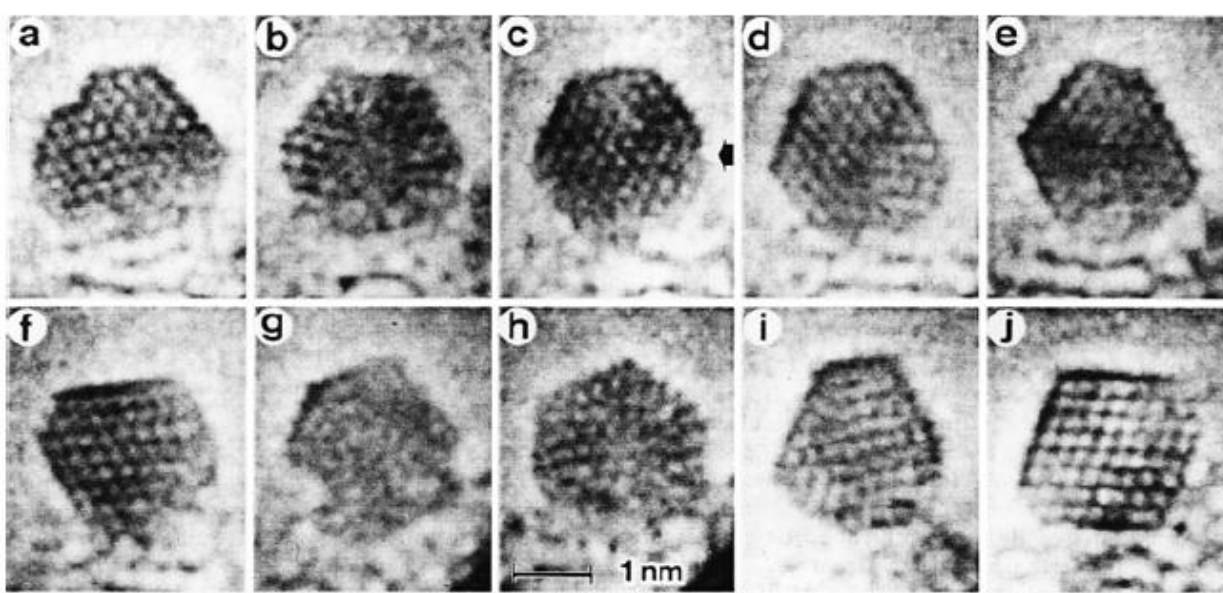


Fig. 7.1. *Upper*: High resolution electron microscope image of a cubo-octahedral cobalt cluster with hexagonal faces, containing roughly 1 000 atoms [2]. *Lower*: Representation of the same polyhedron



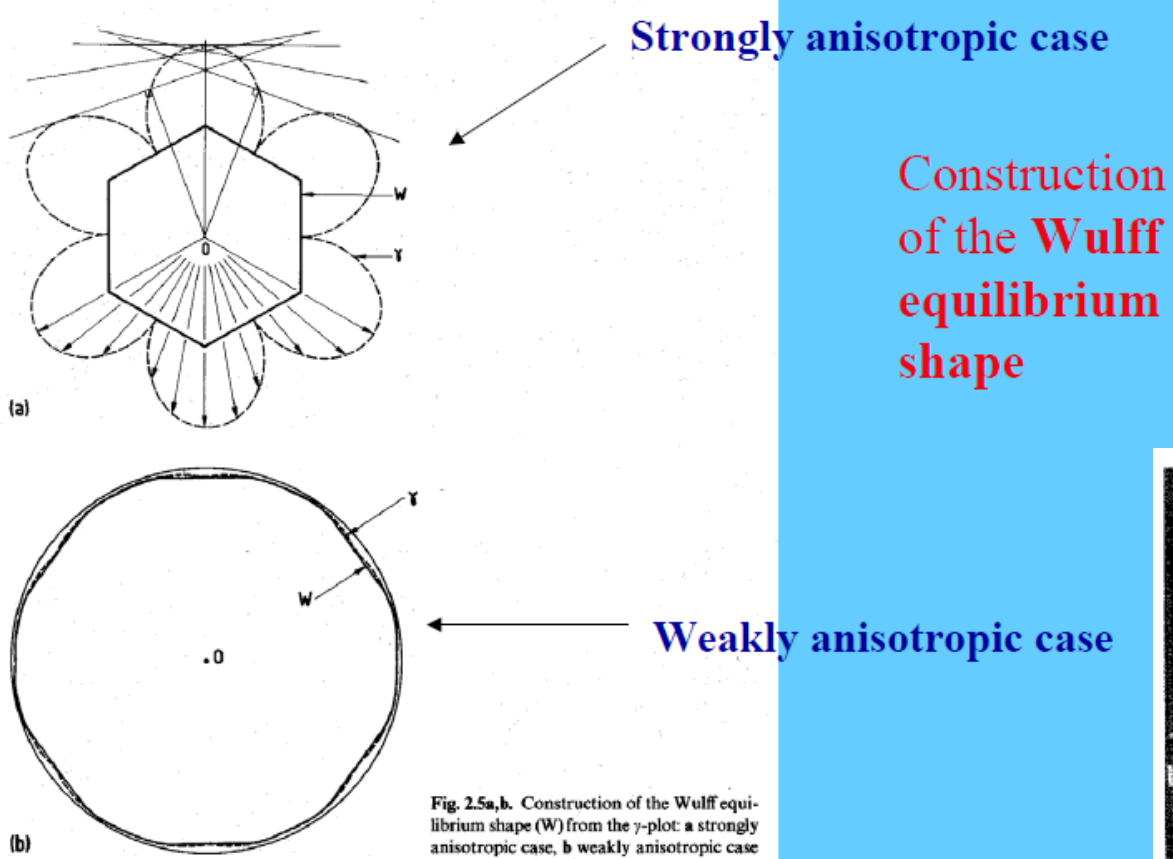
Defects introduction

Fig. 1.7. High-resolution electron microscope images of a 2-nm gold cluster comprising 459 atoms. The structure fluctuates during the observation period. The particle changes between an fcc truncated octahedral shape [(e), (f), and (j)], a polyhedron with fcc structure and a twinned structure [(a), (d), and (i)], and a multitwinned icosahedral structure [(b) and (h)]. Taken from Iijima and Ichihashi [15] with kind permission of the American Physical Society ©1986

For clusters with a number of atoms intermediate between two consecutive closed shells, the shape can be different and it may even oscillate between shapes with fivefold symmetry (icosahedron, decahedron) and shapes corresponding to an fcc structure [14]. In any case, it should be noted that the energy difference between the various structures for very small clusters is actually very low, so that in practice, at finite temperatures, a range of shapes is observed. In situ electron microscope observations show that the shape of small metallic particles fluctuates incessantly between different structures, passing through disordered structures. Figure 1.7 shows a series of high-resolution

Thermodynamics+Kinetics Effects

$T > 0 \text{ K}$



Equilibrium shapes of Pb crystals at selected T 's

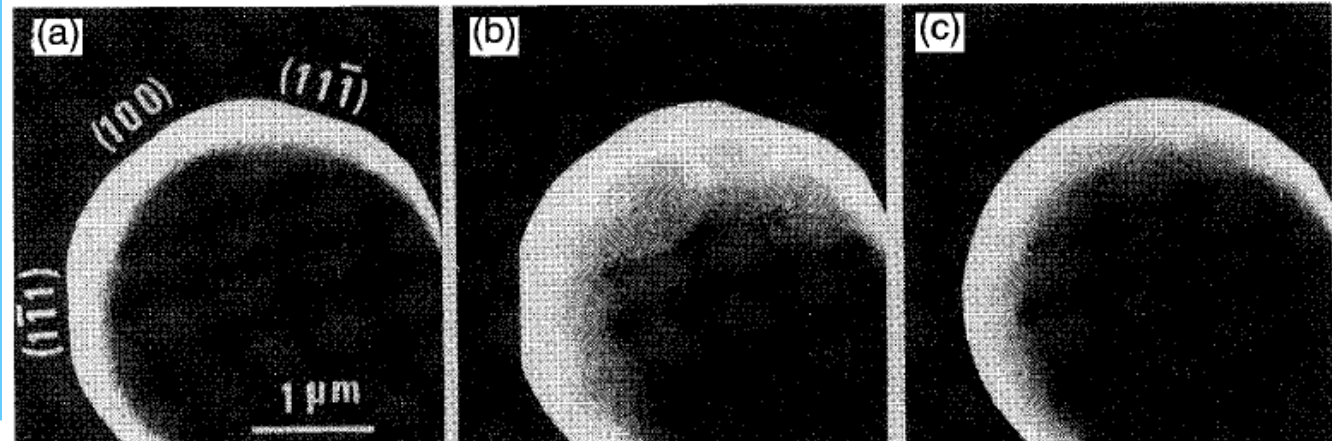
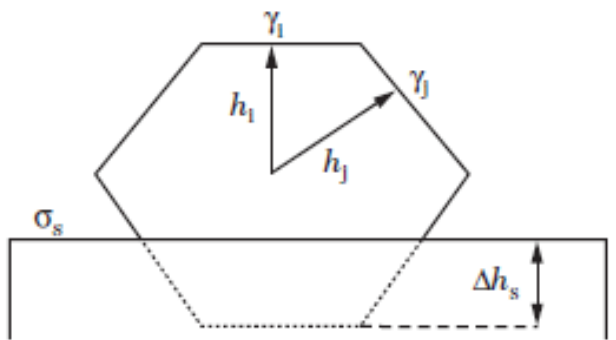


Figure 1.7. SEM photographs of the equilibrium shape of Pb crystals in the [011] azimuth, taken *in situ*: (a) at 300 °C, (b) at 320 °C, showing large rounded regions at 300 °C, and missing orientations at 320 °C; (c) at 327 °C where Pb is liquid and the drop is spherical (from Métois & Heyraud 1989, reproduced with permission).

Morphology of Supported Particles

Wulff–Kaichew Theorem



$$\frac{\Delta h_s}{h_i} = \frac{E_{adh}}{\gamma_i}$$

Fig. 1.12. Schematic representation of the equilibrium shape of a supported crystal. In equilibrium, the crystal interacting with the substrate assumes the form of the Wulff polyhedron (of the free crystal), truncated at the interface to a height of Δh_s . Taken from Henry [20]

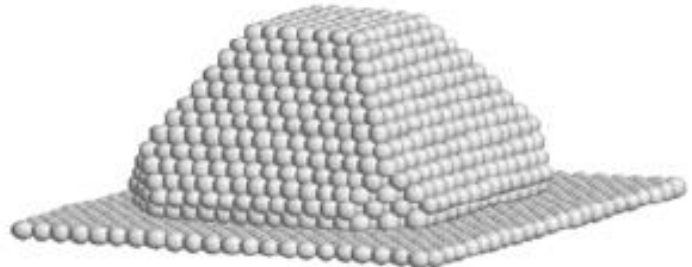


Fig. 1.14. Molecular dynamics simulation for Pd/MgO (100). Equilibrium shape of a 5-nm cluster. Taken from Vervisch et al. [23]

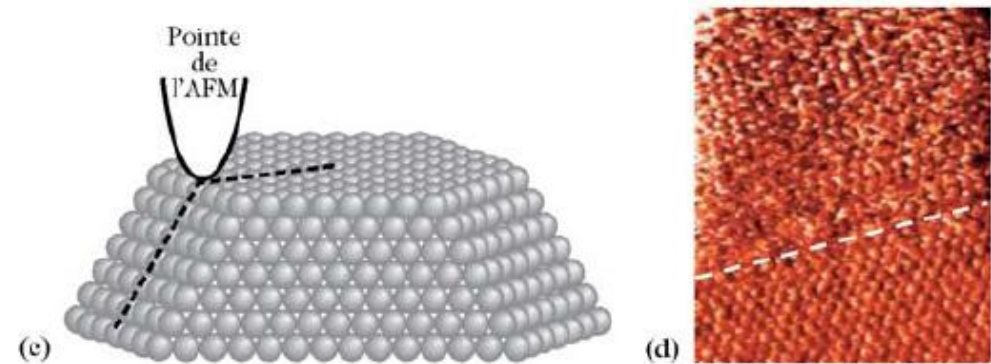
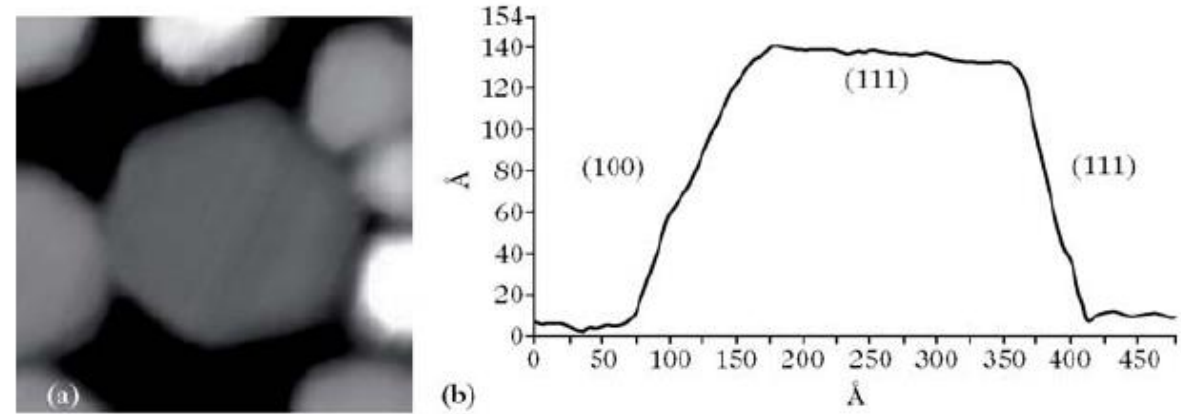
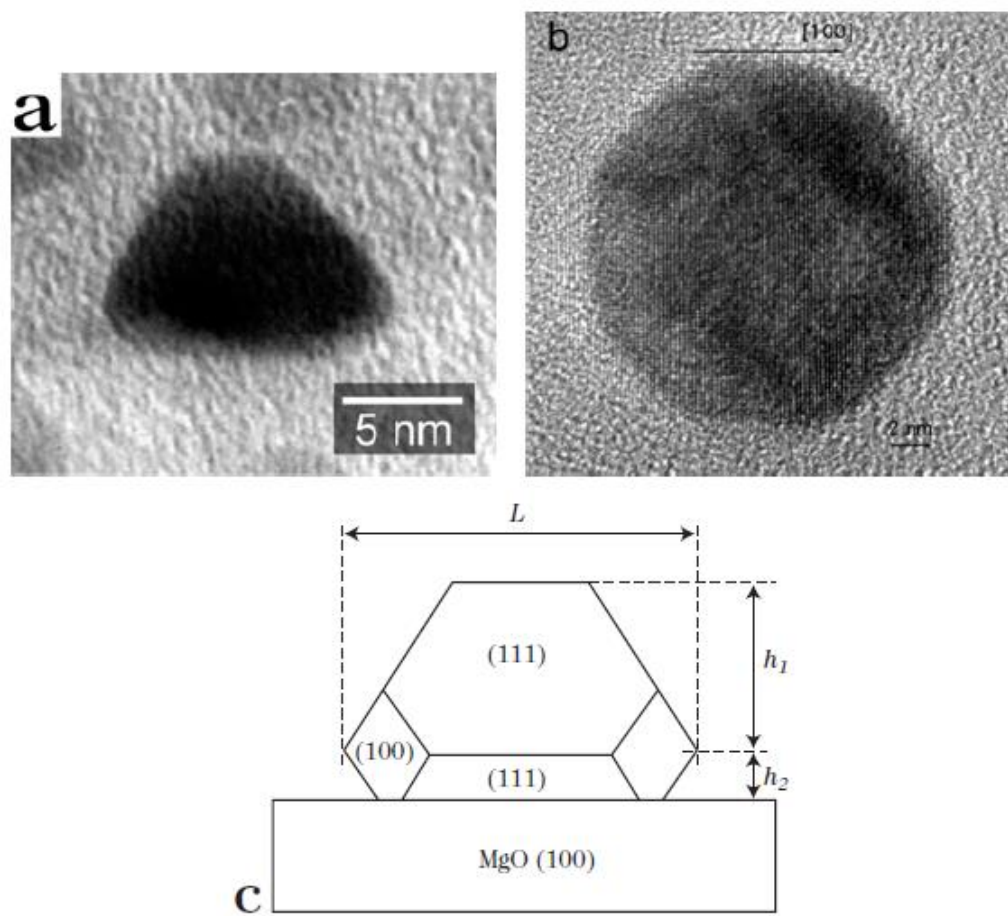


Fig. 1.18. Equilibrium morphology of Pd clusters grown epitaxially on MgO (100). (a) Side view of a 10-nm cluster in a $\langle 110 \rangle$ direction, obtained by TEM on a folded carbon replica. (b) HRTEM image of a 17-nm Pd particle, visualising $\{200\}$ atomic planes separated by 0.2 nm. (c) Equilibrium shape (schematic) of Pd particles with a size of at least 10 nm, grown epitaxially on MgO (100). The observation direction is $\langle 100 \rangle$. Taken from Graoui et al. [25] with kind permission of Elsevier, and Prévot et al. [26]

$$\frac{\Delta h_s}{h_i} = \frac{E_{adh}}{\gamma_i} \quad \longrightarrow \quad E_{adh} = 0.85 \text{ J/m}^2$$

Inverse Wulff Construction

Crystal growth

The **Wulff theorem** can be run in reverse to determine the **anisotropy** of the **surface tension**.

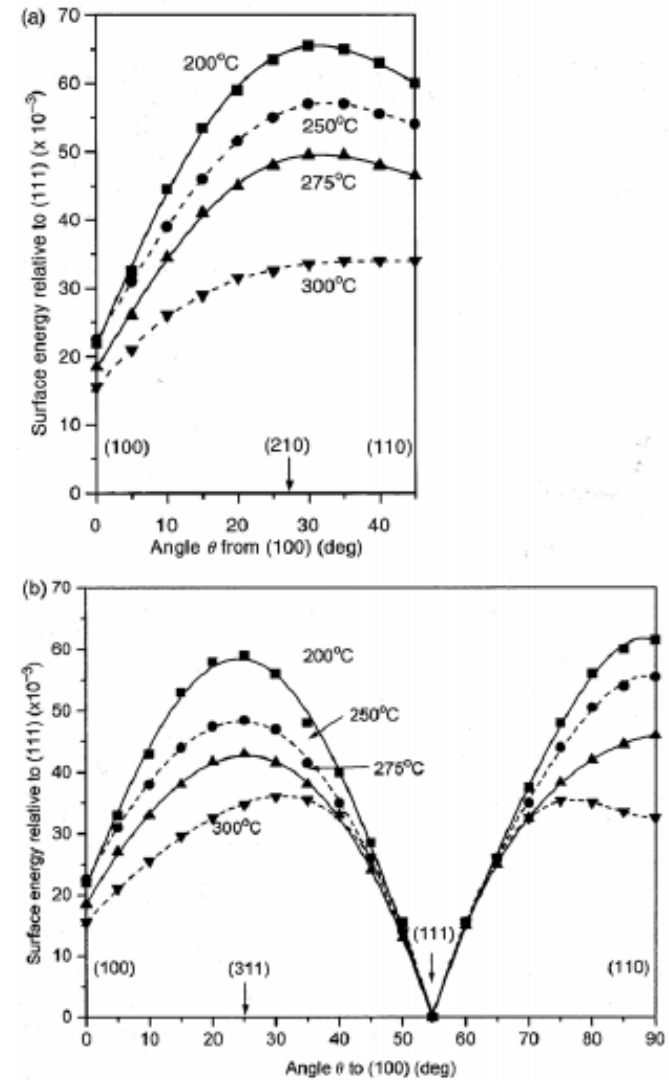


Figure 1.8. Anisotropy of $\gamma(\theta)$ for Pb as a function of temperature, where the points are the original data, with errors $\sim \pm 2$ on this scale, and the curves are fourth-order polynomial fits to these data: (a) in the (100) zone; (b) in the (110) zone. The relative surface energy scale is $(\gamma(\theta)/\gamma(111) - 1) \times 10^{-3}$, so 70 corresponds to $\gamma(\theta) = 1.070 \times \gamma(111)$ (after Heyraud & Métois 1983, replotted with permission).

Nanoscale Res Lett (2007) 2:240–247

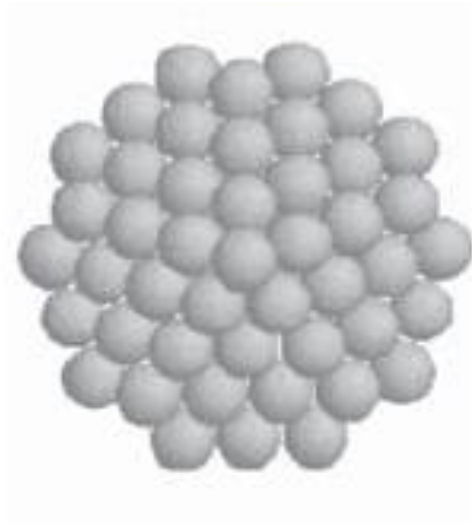
DOI 10.1007/s11671-007-9058-4

NANO EXPRESS

Effect of surrounding environment on atomic structure and equilibrium shape of growing nanocrystals: gold in/on SiO₂

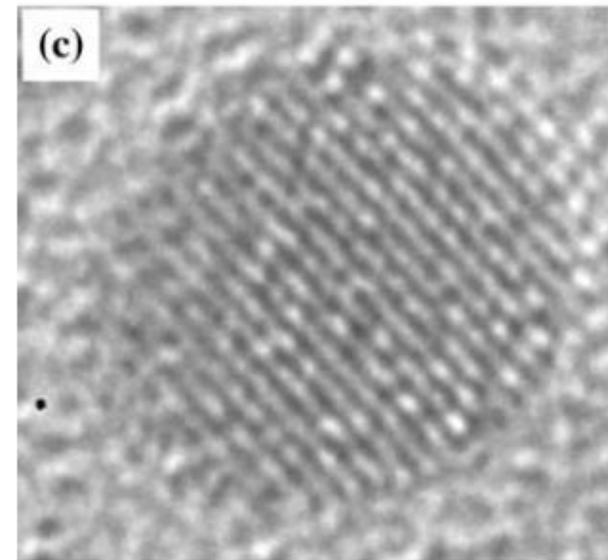
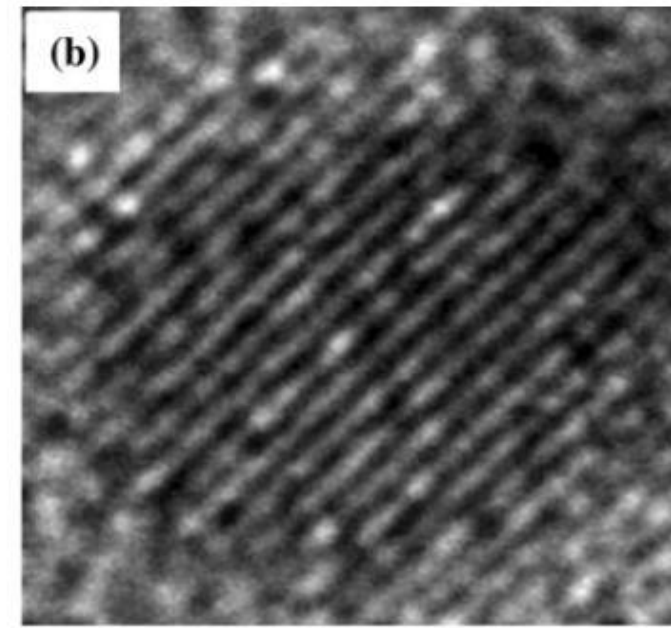
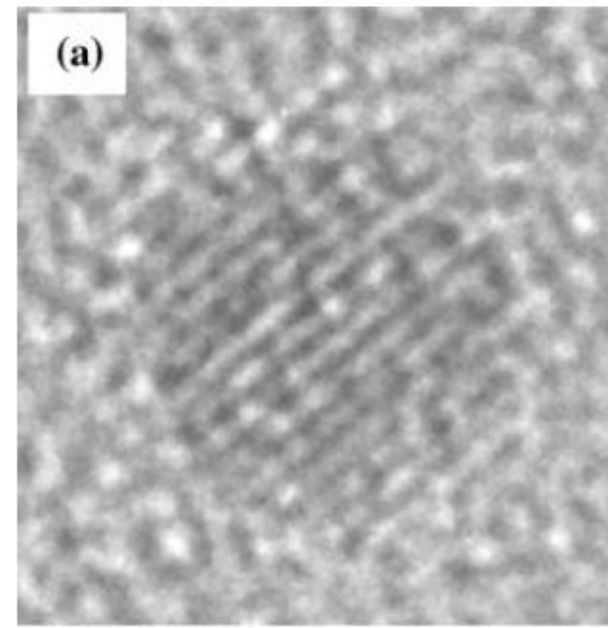
**F. Ruffino · C. Bongiorno · F. Giannazzo ·
F. Roccaforte · V. Raineri · M. G. Grimaldi**

Fig. 2 HR-TEM images of Au NCs in SiO₂ with the same size as the NCs on SiO₂ forming the three determined groups



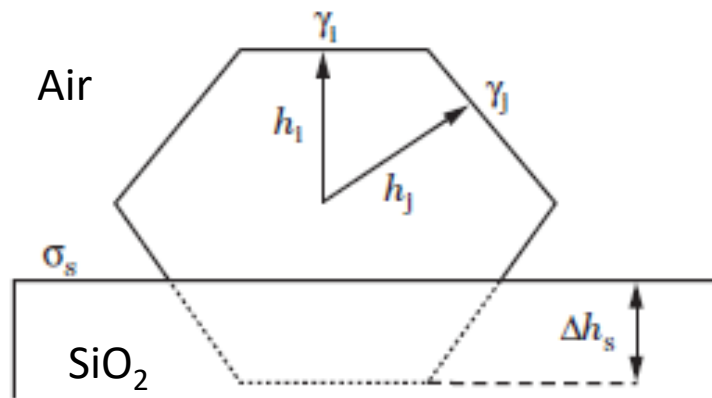
SiO₂

Embedding: isotropic condition

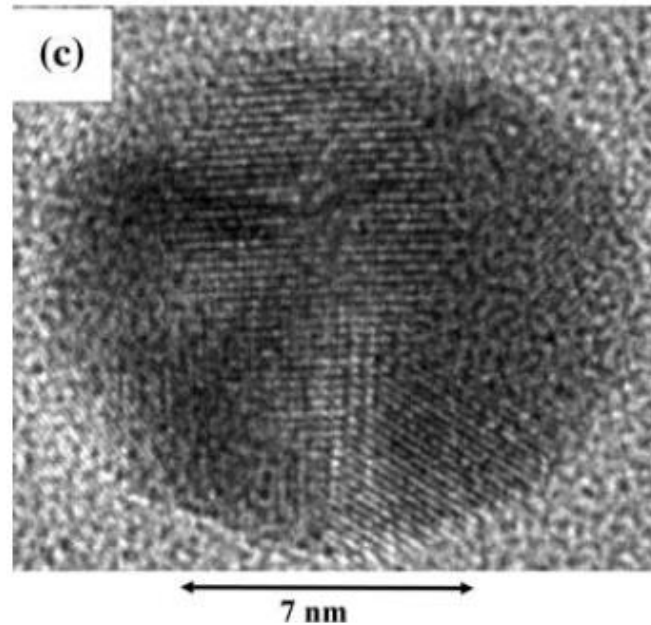
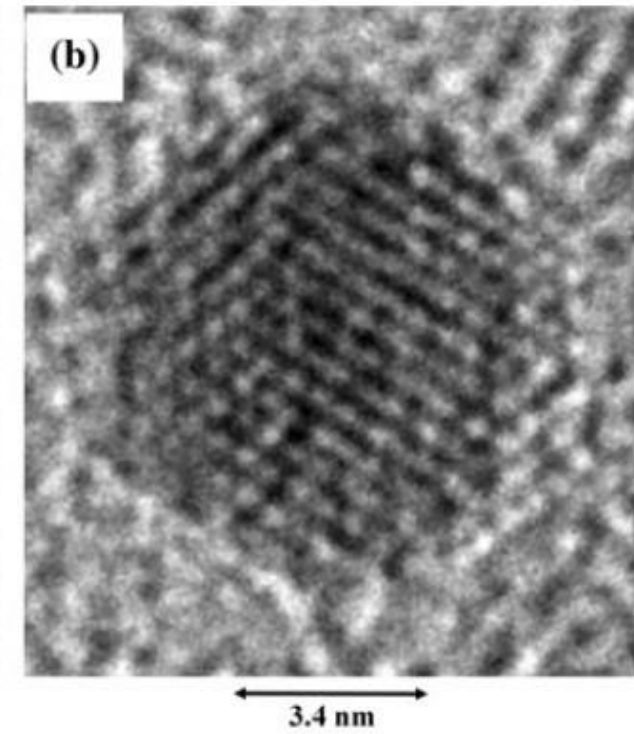
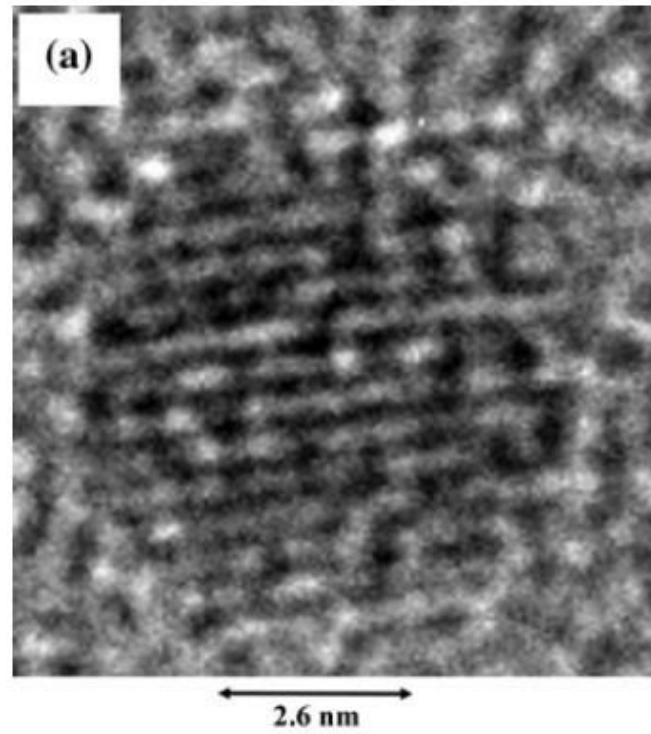


6.8 nm

Fig. 3 HR-TEM images of Au NCs on SiO₂ for the three determined groups ((a) relative to the group 1, (b) to the group 2 and (c) to the group 3)



On substrate: non-isotropic condition



$$\frac{\gamma_i}{h_i} = \text{constant}$$

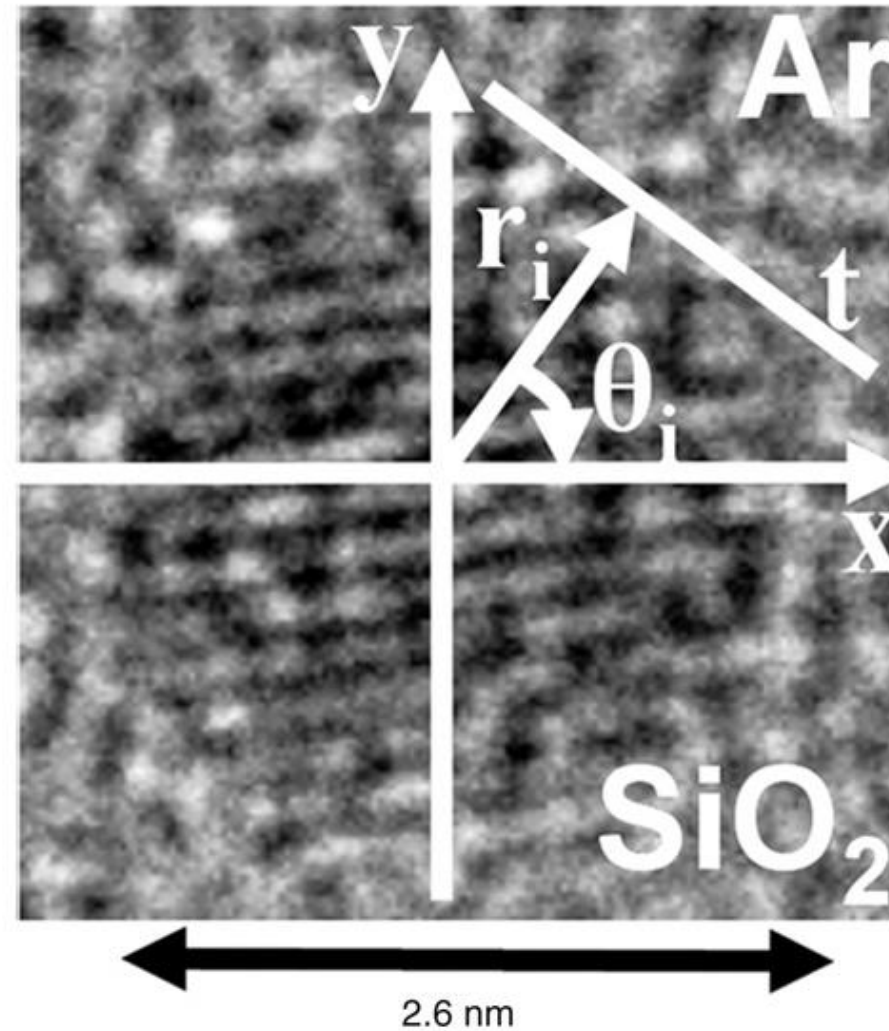
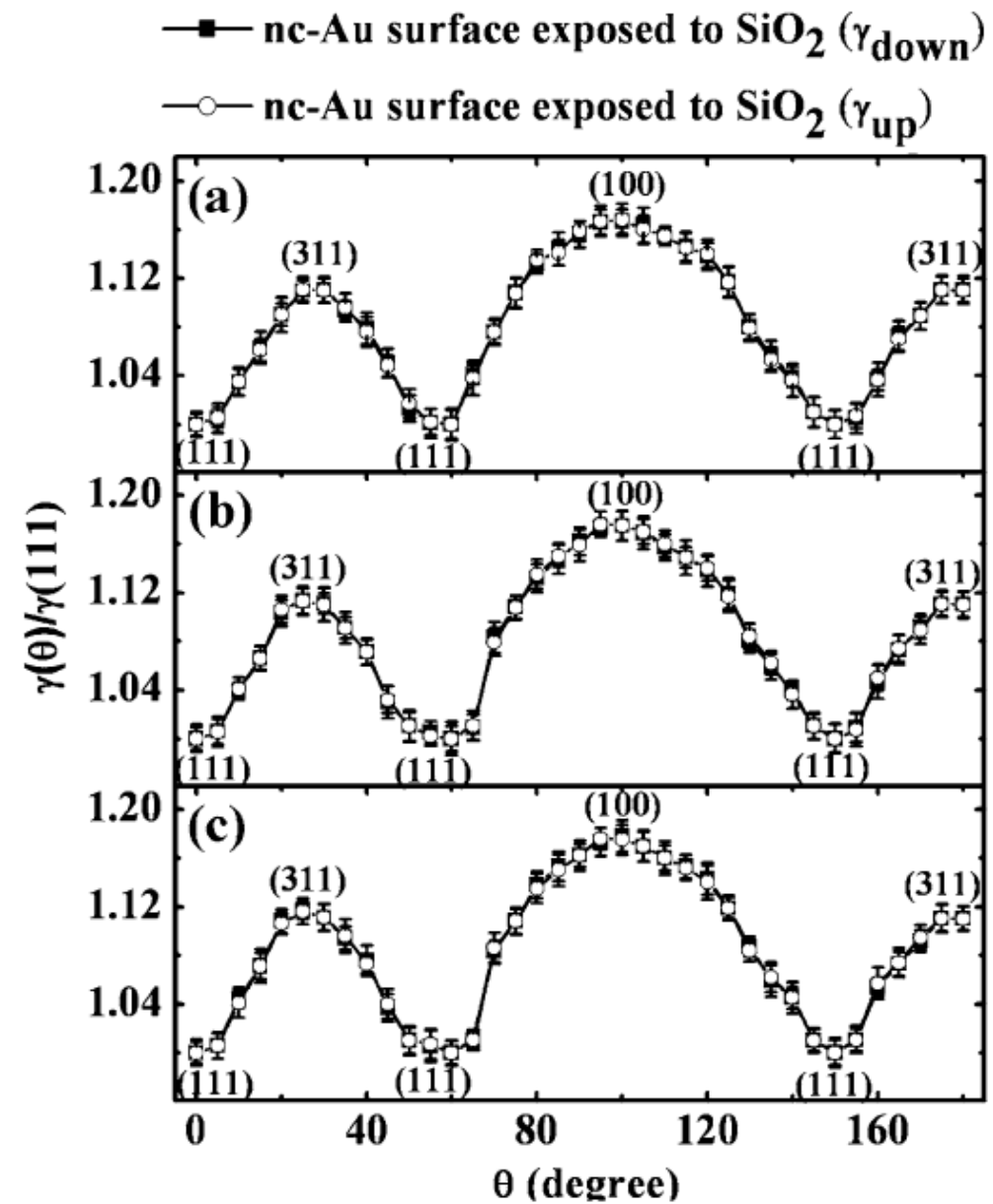
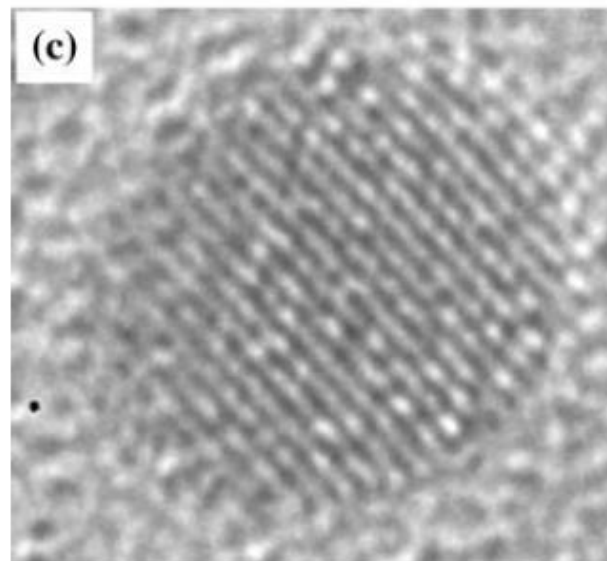
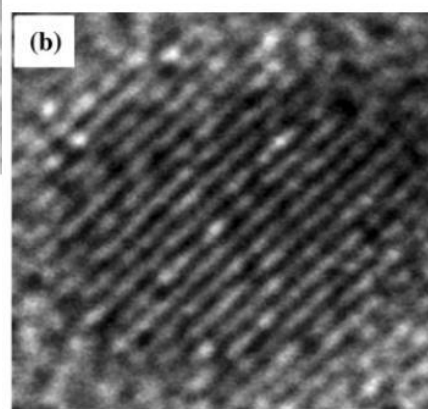
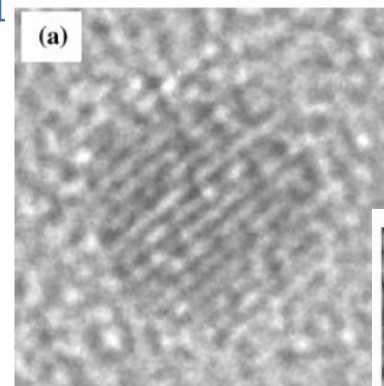
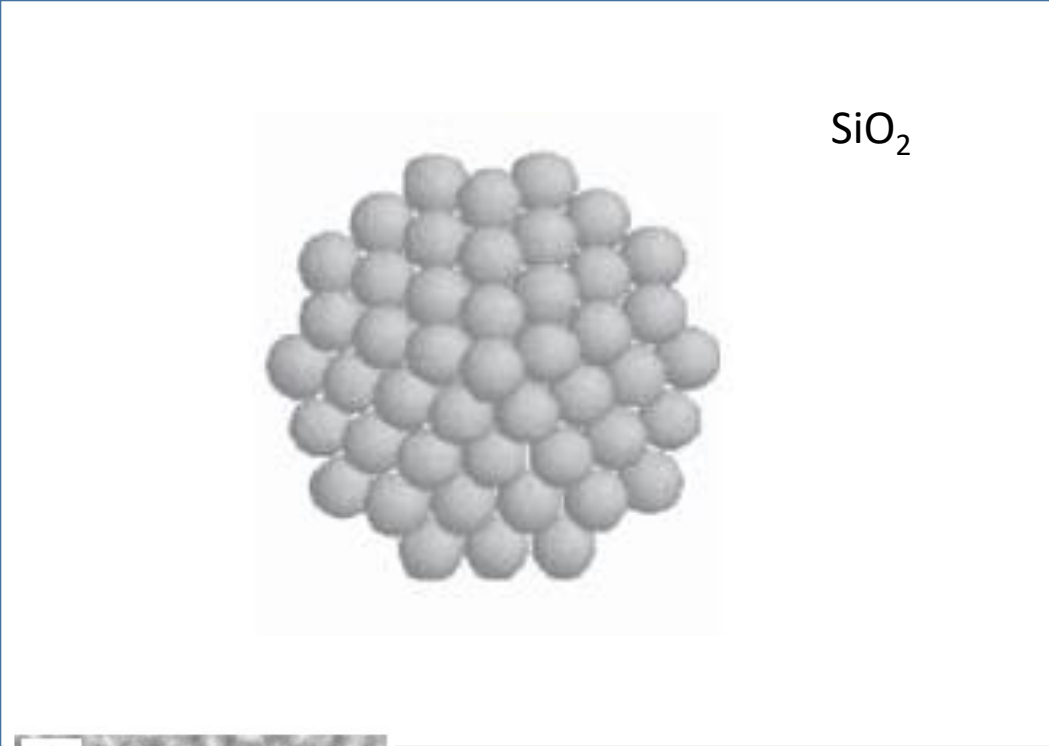
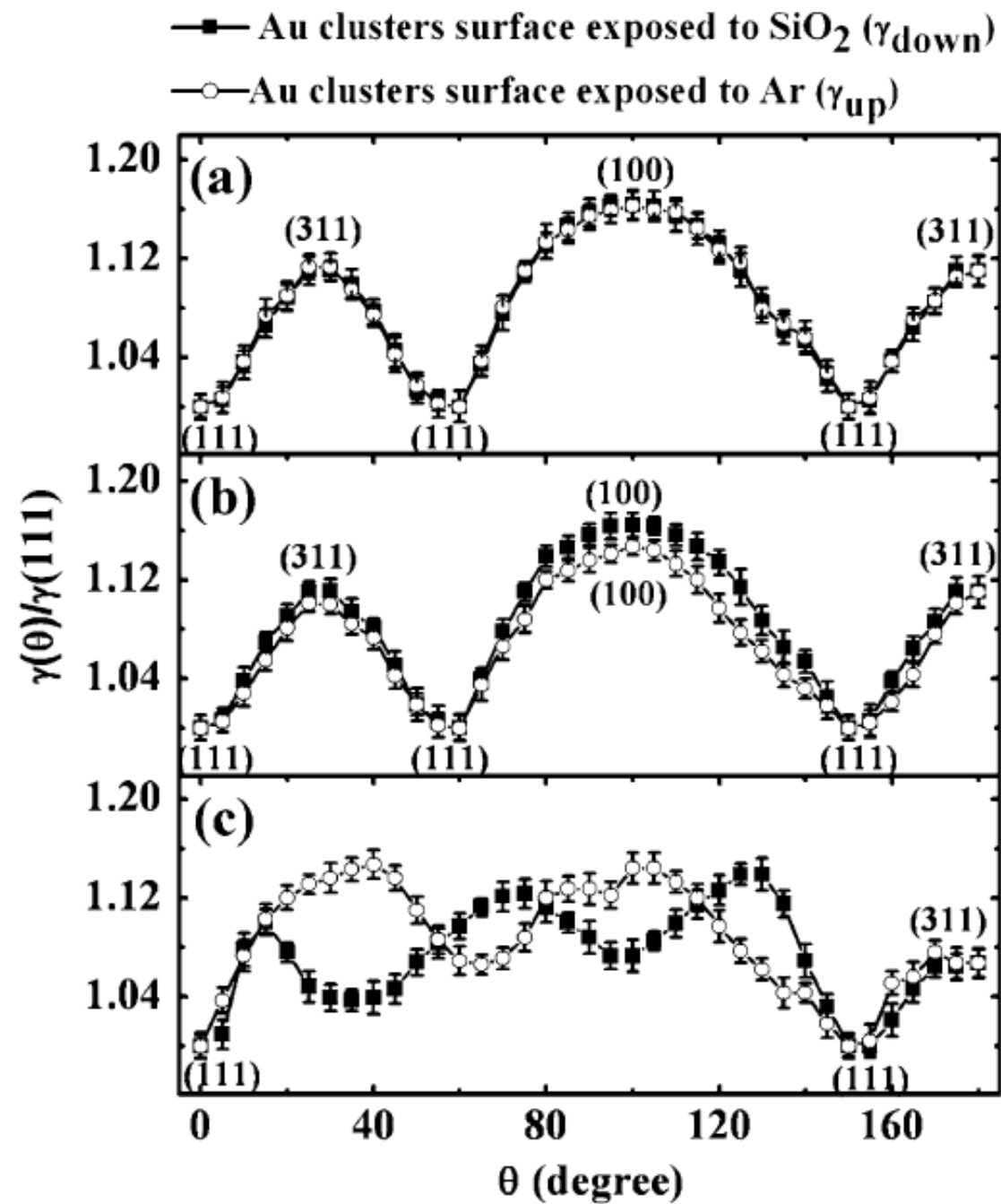
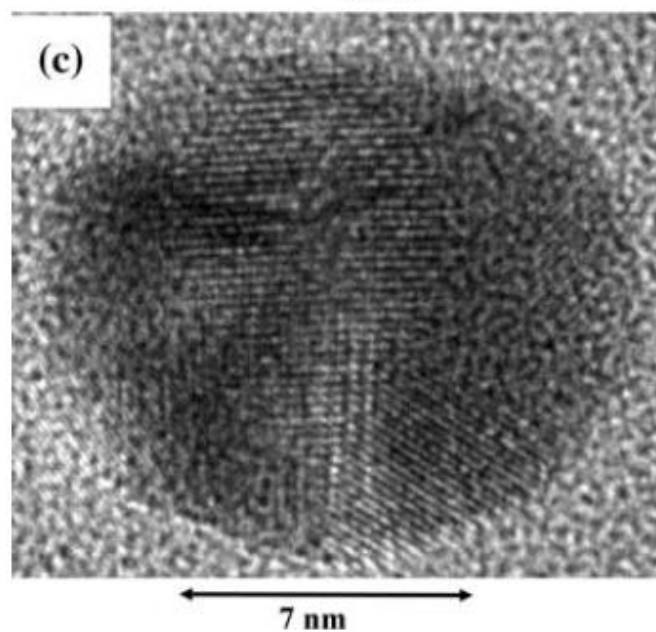
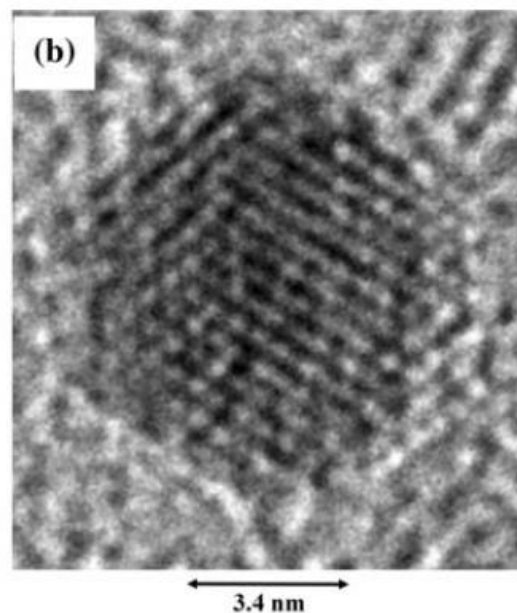
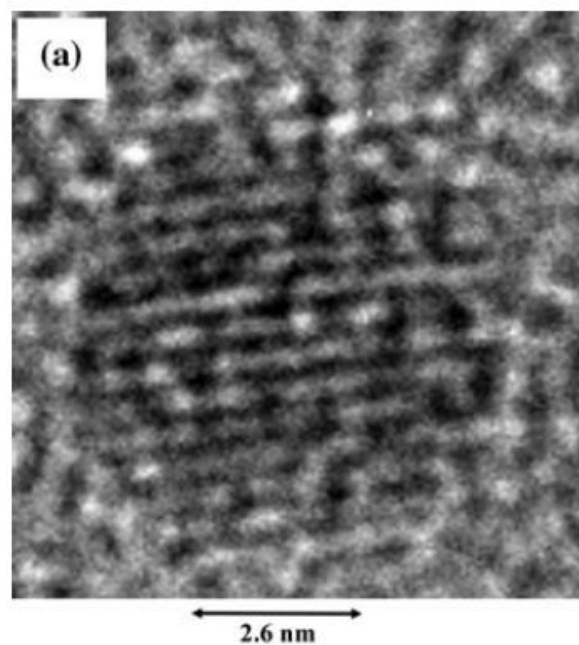
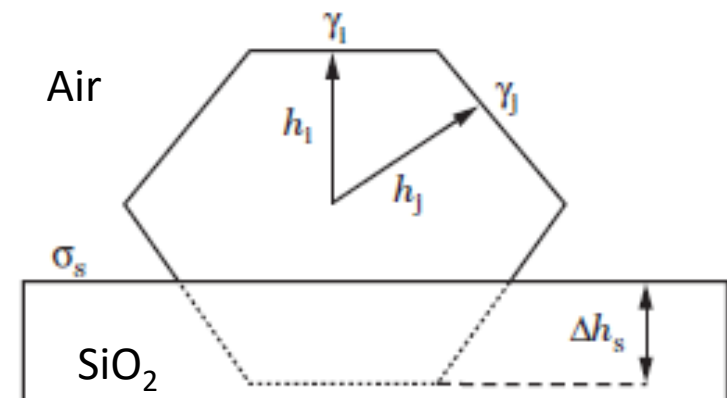


Fig. 6. Schematic of how the inverse Wulff construction was performed; (r, θ) is the polar plot associated to the (x, y) Cartesian plot with origin on the Wulff centre of the NC, t is the tangent to the NC surface along the θ_i direction, r_i the distance between this tangent and the Wulff centre.





(Size-dependent) Melting of Nanostructures (Solid-Liquid Transition)

- A size effect, or confinement effect. The nanograin behaves like a kind of box, within which the property may or may not exist [1]. Below a certain critical size, characteristics of the property depend on the grain size. This is the size or confinement effect. The way these characteristics change as a function of size is often non-monotonic and can exhibit extrema.
- A surface or interface effect. In the nanograin, the contribution from layers close to the surface occupies a more and more important place in the overall behaviour of the material as the grain size decreases [1]. The surface energy gradually becomes the dominating contribution to the total energy of the material. Such a property will evolve monotonically with size and can be treated within the framework of thermodynamics.

Size Dependence of the Solid–Liquid Transition

From the Macroscopic to the Nanometric

The Macroscopic Solid–Liquid Transition. Generalities

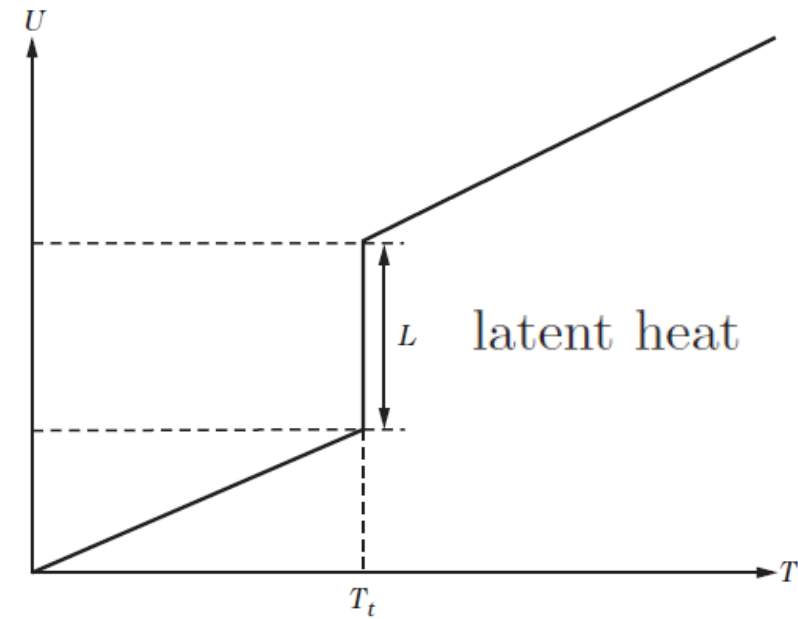
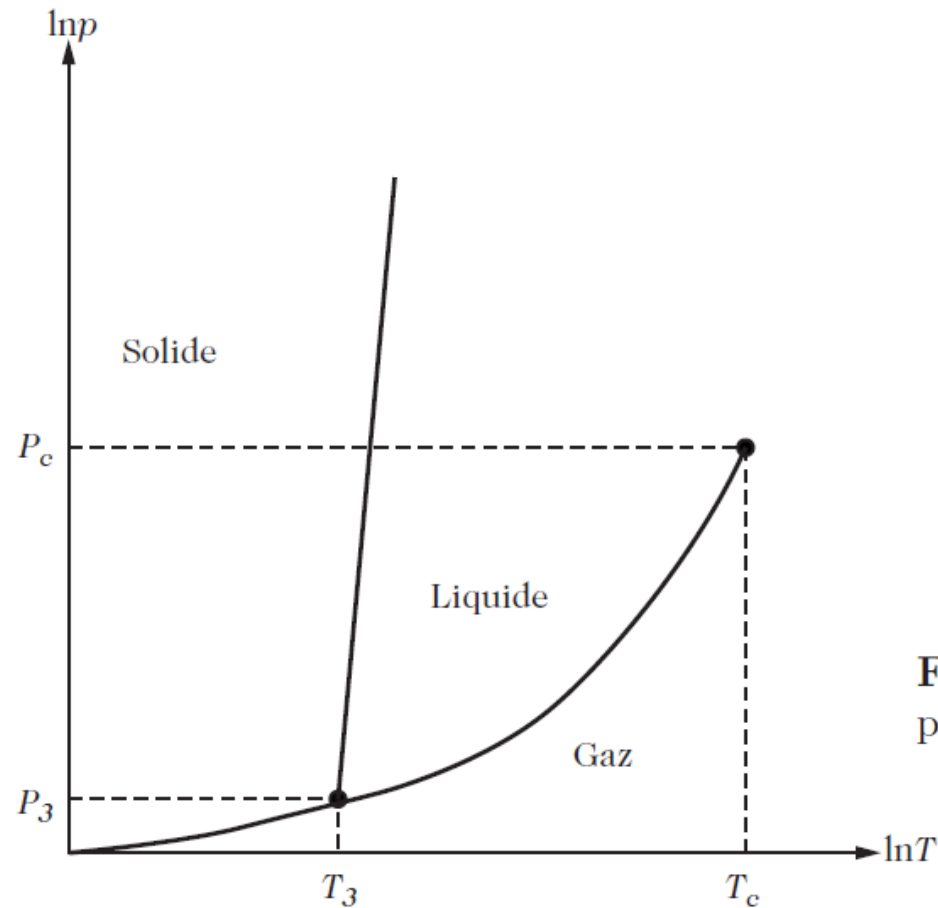


Fig. 3.2. Schematic caloric curve for a simple body at constant volume. Low temperature quantum effects are not represented

Fig. 3.1. Schematic phase diagram of a simple body

Microscopic Theory of the Solid–Liquid Transition

At the present time, there is no satisfactory microscopic theory of the solid–liquid transition. Although it is not a recent discovery, the Lindemann criterion provides a simple and fairly reliable estimate of the melting temperatures of monatomic solids such as metals and noble gases. The key idea is that the amplitude of vibration of atoms in the crystal about their equilibrium position will increase with temperature. When this amplitude reaches a certain fraction f of the distance between nearest neighbours in the crystal lattice, the solid can no longer maintain its crystal structure and it subsequently melts. Experimentally, it is observed that for all monatomic solids $f \simeq 0.07$ [2]. In order to apply this to nanoparticles, we shall state this criterion in the form: a monatomic solid melts when the fluctuations in interatomic distances are of the order of 14%. Indeed, bond length fluctuations are equal to twice the vibrational amplitude of atoms located at each end of the bond. These fluctuations are given by the relative squared deviation δ defined by

Amplitude of atomic vibrations

$$\delta = \frac{2}{N(N-1)} \sum_{i < j} \frac{\sqrt{\langle r_{ij}^2 \rangle - \langle r_{ij} \rangle^2}}{\langle r_{ij} \rangle}, \quad (3.1)$$

where $\langle \rangle$ stands for a time average and r_{ij} is the distance between atoms i and j . δ is in fact also an average over all bonds of the relative fluctuation of each bond.

The solid–liquid transition is characterised by two thermodynamic parameters: the transition temperature T_t and the latent heat L . The Lindemann criterion provides a phenomenological prediction of the melting temperature, viz., the solid melts when the relative fluctuation in the interatomic distances reaches about 14%.

Size Effects on the Solid–Liquid Transition

The distinction between solid and liquid is obvious on our scale, in the sense that we can see immediately whether a glass of water is frozen or not. However, if we think about this for a moment, it is not so easy to find measurable criteria capable of distinguishing between the two states. An elementary school book gives the following definition: a liquid adopts the shape of the container in which it is held. But it would be hard to transpose this idea to the nanoscale!

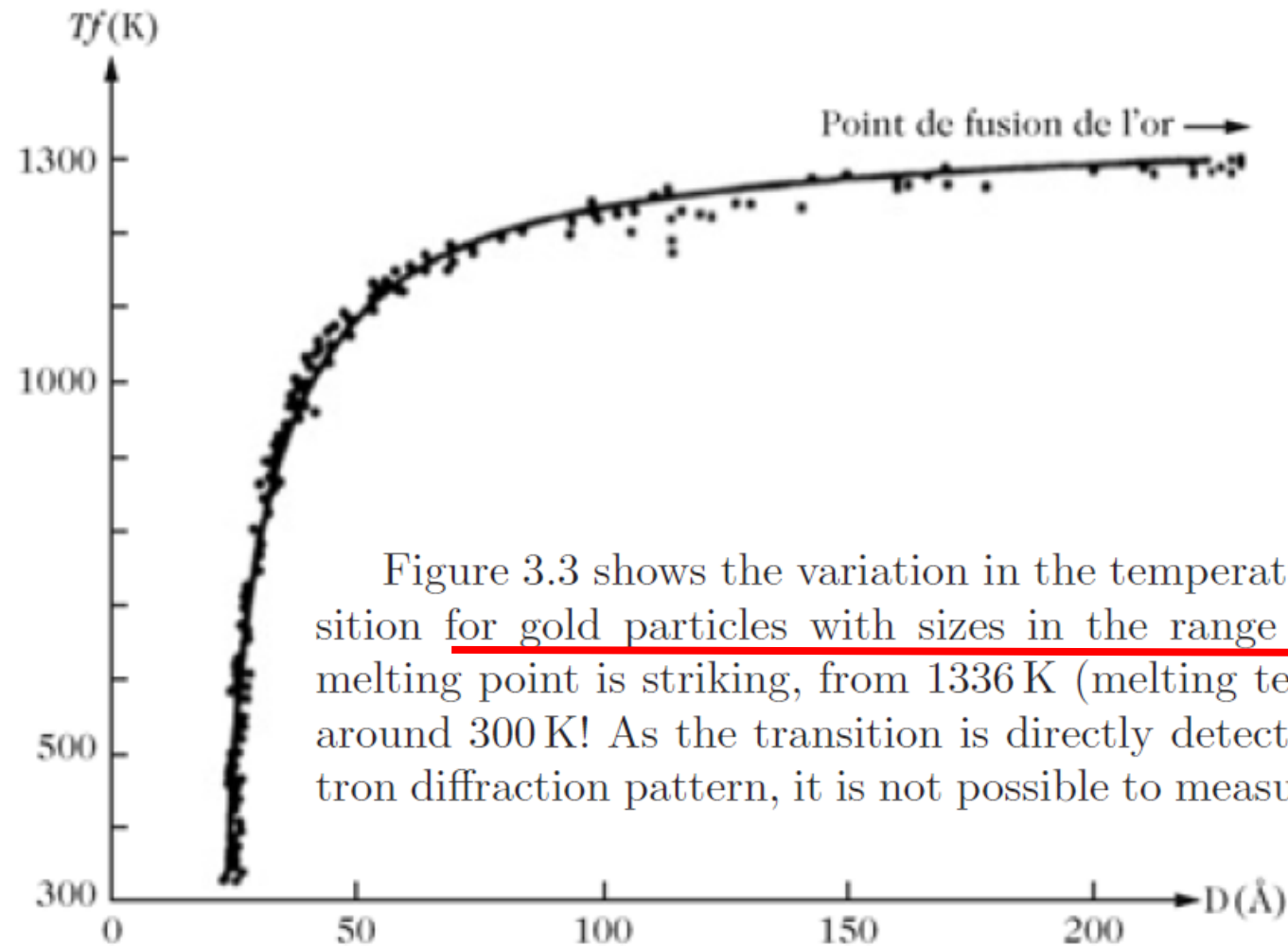


Figure 3.3 shows the variation in the temperature of the solid–liquid transition for gold particles with sizes in the range 2–25 nm. The drop in the melting point is striking, from 1336 K (melting temperature of solid gold) to around 300 K! As the transition is directly detected by a change in the electron diffraction pattern, it is not possible to measure the latent heat. This has

Fig. 3.3. Dependence of the solid–liquid transition temperature of gold on particle diameter. Taken from [4]. The transition is detected by the disappearance of Bragg peaks in the electron diffraction pattern. *Dots* represent experimental values. The *continuous curve* is fitted to (3.3) by the least squares method

Classical Models

In order to model a small particle, surface effects cannot be ignored. The first effect due to the presence of a surface is to add a surface tension term to the thermodynamic potentials. If this correction is taken into account, assuming furthermore that the thermodynamic parameters do not depend on the size, the so-called classical models for the melting of small particles are obtained.

All these theories are based on the Gibbs–Duhem equation, expressing the chemical potentials of the solid and the liquid, and the Laplace equation for the surface, taking surface tension into account. A first order expansion gives an expression of the form

$$v_{\text{LJ}}(r) = e_0 \left[\left(\frac{r_0}{r} \right)^{12} - 2 \left(\frac{r_0}{r} \right)^6 \right] \quad 1 - \frac{T_m(r)}{T_m(\infty)} = \frac{2\alpha}{\rho_s L(\infty)r}, \quad (3.2)$$

where $T_m(r)$ is the melting temperature of the particle of radius r , $T_m(\infty)$ is the melting temperature of the bulk solid, ρ_s is the density of the solid,

$L(\infty)$ is the latent heat of fusion of the bulk solid, and α is a function of the solid–liquid surface tension γ_{sl} , the solid–vapour surface tension γ_s , and the liquid–vapour surface tension γ_l .

Surface-area-difference model for thermodynamic properties of metallic nanocrystals

W H Qi^{1,2}, M P Wang², M Zhou¹ and W Y Hu³

The surface-area-difference (SAD) model is developed for the cohesive energy of metallic crystals by taking into account surface effects, and has been extended to predict the thermodynamic properties of metallic nanoparticles, nanowires and nanofilms with free and non-free surfaces (embedded in a matrix). It is found that the thermodynamic properties of metallic nanocrystals depend on the crystal size and the interface coherence, where the interface coherence determines the variation tendency (increasing or decreasing), and the size determines the magnitude of the variation. The present calculated results on the thermodynamic properties of metallic nanocrystals by the SAD model are consistent with the corresponding experimental values.

To give more general formulae of the SAD model, we assume that the crystal is embedded in a matrix. If the crystal consists of n atoms, the total surface area of n atoms is $n \cdot 4\pi r^2$, and the corresponding surface energy is $n \cdot 4\pi r^2 \cdot \gamma_0$, where r is the atom radius and γ_0 is the surface energy of the crystal per unit area at 0 K. If each interface atom contributes half its surface to the interface area of the crystal, the interface energy of the crystal is $N \cdot 2\pi r^2 \cdot \gamma_i$, where N is the number of interface atoms and γ_i is the interface energy per unit area at 0 K. Then, the increased surface energy after dividing the crystal into isolated atoms, i.e. the cohesive energy of the crystal, can be written as

$$\begin{aligned} E_n &= n \cdot 4\pi r^2 \gamma_0 - N \cdot 2\pi r^2 \gamma_i \\ &= n \cdot 4\pi r^2 \cdot \gamma_0 \left(1 - \frac{N}{2n} \cdot p \right), \end{aligned} \quad (1)$$

where $p = \gamma_i/\gamma_0$, and γ_i can be computed using the surface energy of the crystal and that of the matrix [5]. By considering the coherence (the coherence is used to describe the lattice matching of the interface atoms between the matrix and the nanocrystals), we have $\gamma_i = \gamma_0 - q\gamma_M$, where γ_M denotes the surface energy of the matrix per unit area at 0 K, and q denotes the coherence between the crystal and the matrix. $q = 1$ is the coherent interface, $q = 0.5$ the semi-coherent interface, and $q = 0$ is the non-coherent interface. The case of $q = 0$ is the same as that of the crystal with the free surface.

The cohesive energy per atom is $E = E_n/n$, i.e.

$$E = E_b \left(1 - \frac{N}{2n} \cdot p \right), \quad (2)$$

where $E_b (= 4\pi r^2 \cdot \gamma_0)$ is the cohesive energy per atom of the crystal neglecting the boundary conditions. In other words, we have $E = E_b$ by ignoring the interface effect. E can be regarded as the interface dependent cohesive energy. Since there is no size limit in its expression, equation (2) can be

Crystal structure

The number of atoms per unit volume is denoted as ρ_V , and the number of atoms per unit area in the plane (hkl) is denoted as ρ_S . For a layer of a crystal plane, the number of atoms per unit area equals that of the volume $d_{hkl} \cdot 1$, where d_{hkl} is the interplanar distance of (hkl) , and d_{hkl} can be computed using the lattice constants. For example, for the cubic crystal, we have $d_{hkl} = a / \sqrt{h^2 + k^2 + l^2}$ (a is the lattice parameter). Then, we have

$$\rho_S = \rho_V \cdot d_{hkl}. \quad (3)$$

The number of total atoms is $\rho_V \cdot V$, and the number of interface atoms is $\sum_K \rho_{SK} \cdot S_K$, where ρ_{SK} is the number of atoms per unit area in the plane K , and S_K is the area of the plane K . Sigma denotes the sum of the contributions of all interface atoms in different planes. Then, the size term in equation (2) can be written as

$$\frac{N}{n} = \frac{\sum_K \rho_{SK} \cdot S_K}{\rho_V \cdot V}. \quad (4)$$

Application of the SAD model to nanocrystals

We assume that all the interfaces of a spherical nanoparticle have the same plane index, and then the term $p \cdot \sum_K \rho_{SK} \cdot S_K / (2\rho_V \cdot V)$ is reduced to $\rho_S \cdot p \cdot \pi D^2 / (2 \cdot \rho_V \cdot \pi D^3 / 6)$, i.e. $(\rho_S / \rho_V) \cdot 3p / D$, where D is the diameter of the nanoparticle. Taking equation (3) into consideration, we can get the cohesive energy of the spherical nanoparticle (E_P), i.e.

$$E_P = E_b \left(1 - \frac{3pd_{hkl}}{D} \right). \quad (6)$$

Cohesive energy

Equation (5) can also be used to account for the cohesive energy of nanowires and nanofilms embedded in a matrix. Since a nanowire and a nanofilm can be regarded as two limits of a pancake-like nanoparticle, the following discussion is based on a pancake-like nanoparticle, where l and h denote its radius and height, respectively. If $l \ll h$, the pancake-like nanoparticle is a nanowire, and $l \gg h$ is a nanofilm. For simplicity, we still assume that all the interfaces have identical plane indices. For a more rigorous calculation, each plane index should be determined carefully. The volume and the interface area of the pancake-like nanoparticle are $\pi l^2 h$ and $2\pi l h + 2\pi l^2$, respectively. The term $p \cdot \sum_K \rho_{SK} \cdot S_K / (2\rho_V \cdot V)$ can be written as $\rho_S \cdot p \cdot (2\pi l h + 2\pi l^2) / (2 \cdot \rho_V \cdot \pi l^2 h)$, i.e. $(\rho_S / \rho_V) \cdot p \cdot [(2/w) + (1/h)]$, where $w (=2l)$ is the diameter. Then, the corresponding cohesive energy can be written as

$$E = E_b \left[1 - p d_{hkl} \left(\frac{2}{w} + \frac{1}{h} \right) \right]. \quad (8)$$

For a nanowire, we have $w \ll h$. Then, the cohesive energy (E_W) is

$$\text{Nanowire: } w=\text{raggio nanometrico} \quad E_W = E_b \left(1 - \frac{2p d_{hkl}}{w} \right). \quad (9)$$

Correspondingly, for a nanofilm, we have $w \gg h$. The cohesive energy (E_F) is

$$E_F = E_b \left(1 - \frac{p d_{hkl}}{h} \right). \quad (10)$$

Nanofilm: $h=\text{spessore nanometrico}$

This result is the same as that given by the liquid drop model [5]. Equations (7), (9) and (10) can be combined into a unified formula

$$E_j = E_b (1 - p d_{hkl} X_j), \quad (12)$$

where $j (= 0, 1, 2)$ is the low dimension of nanocrystals: $j = 0$ denotes nanoparticles, $j = 1$ nanowires and $j = 2$ nanofilms.

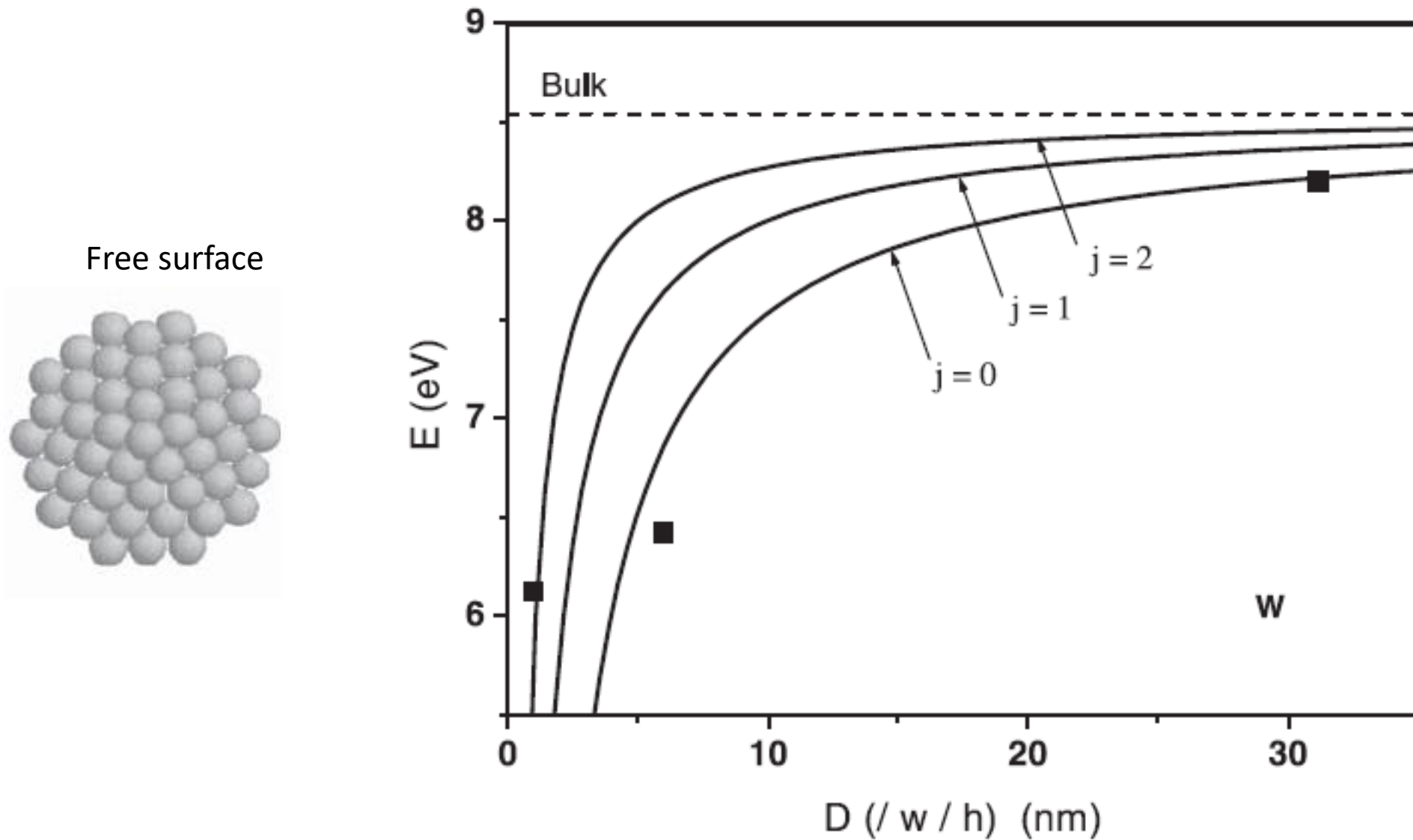


Figure 1. Cohesive energy of W nanocrystals with free surface. The solid lines are calculated by equation (12), where $p = 1$, $d_{100} = 0.31650$ nm [18], $E_b = 8.54$ eV [1] and $\alpha = 1.245$. The symbols '■' denote the experimental values of W nanoparticles [2].

Melting temperature and superheating

Rose *et al* [19, 20] proposed a universal model for solids from the binding theory of solids. Combining their theory with the Debye model, they theoretically derived the well-known empirical relation between the melting temperature and the cohesive energy for pure metals:

$$T_{mb} = \frac{0.032}{k_B} E_b, \quad (13)$$

where T_{mb} is the melting temperature of bulk pure metals and k_B is the Boltzmann's constant. Similar to the cohesive energy, the melting temperature is also a parameter to describe the strength of metallic bonds. Therefore, equation (13) can be regarded as the mathematical conversion of both parameters.

Free surface

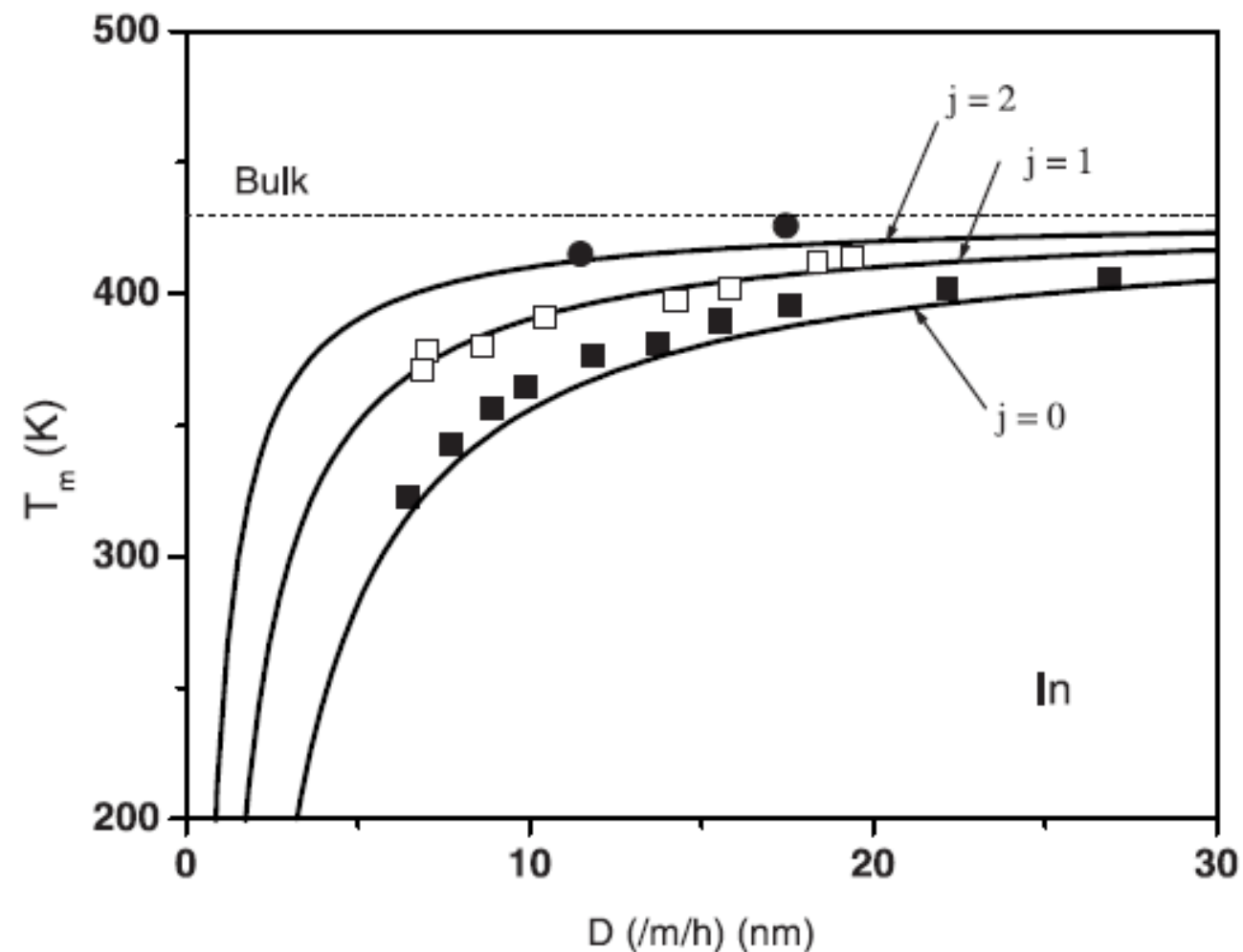
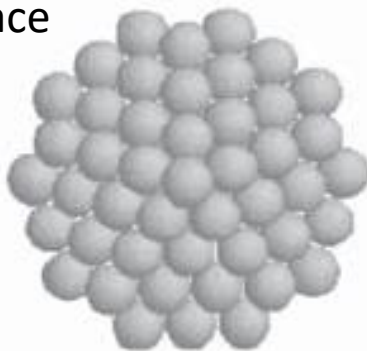


Figure 4. Melting temperature of In nanocrystals with free surface. The solid lines are computed by equation (14), where $p = 1$, $d_{100} = 0.45979$ nm [18], $T_{mb} = 429.8$ K [21] and $\alpha = 1.245$. The symbols '●' [10], '□' [11] and '■' [12] denote the corresponding experimental values of nanofilms, nanowires and nanoparticles.

Melting entropy and melting enthalpy

Ubbelohde [22], Regel and Glazov [23] have shown that the melting entropy (S_{mb}) of a metallic crystal is mainly vibration entropy (S_{vb}). Then, the melting entropy of metallic crystals can be written as

$$S_{mb} = \frac{3}{2}k_B \ln \left(\frac{T_{mb}}{C} \right), \quad (15)$$

where C is a constant. By replacing T_{mb} by T_j , we can obtain the size dependent melting entropy of nanoparticles, nanowires and nanofilms. The expressions are simplified as

Free surface

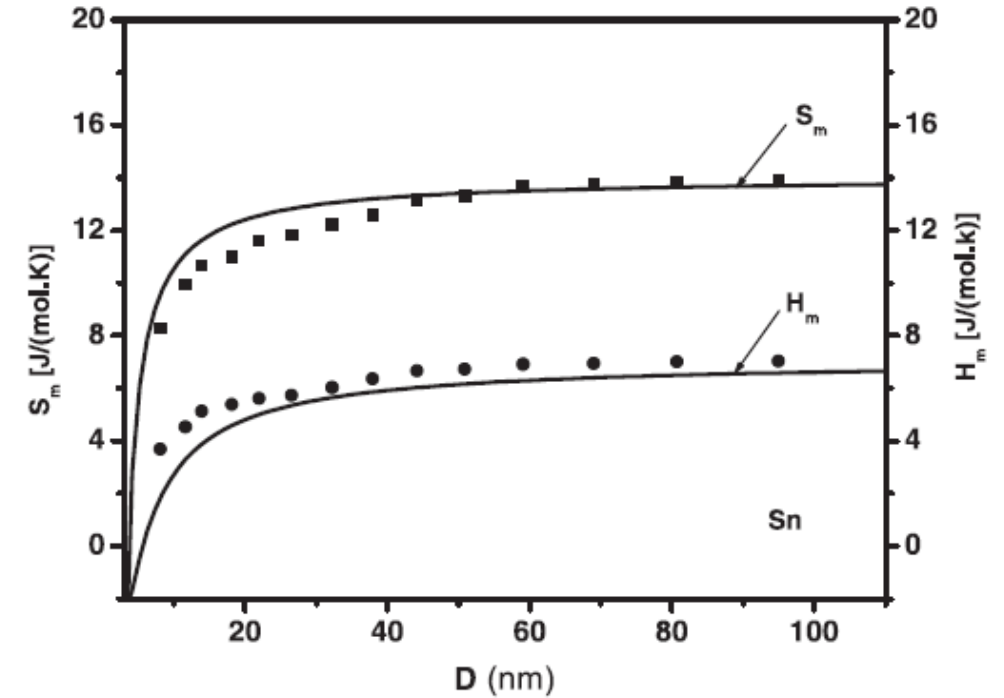
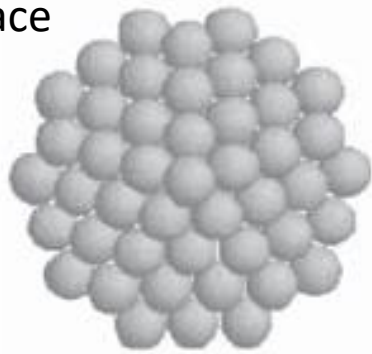


Figure 6. Melting entropy and melting enthalpy of Sn nanocrystals with free surface. The solid lines denote the results calculated by equations (16) and (17), respectively, where $d_{100} = 0.64892$ nm [18], $H_{mb} = 7.08$ J mol⁻¹ K⁻¹ [24], $S_{mb} = 14.02$ [24], $\alpha = 1.245$ and $p = 1$. The symbols '■' and '●' denote the corresponding experimental values [25].

Embedded Nanostructures

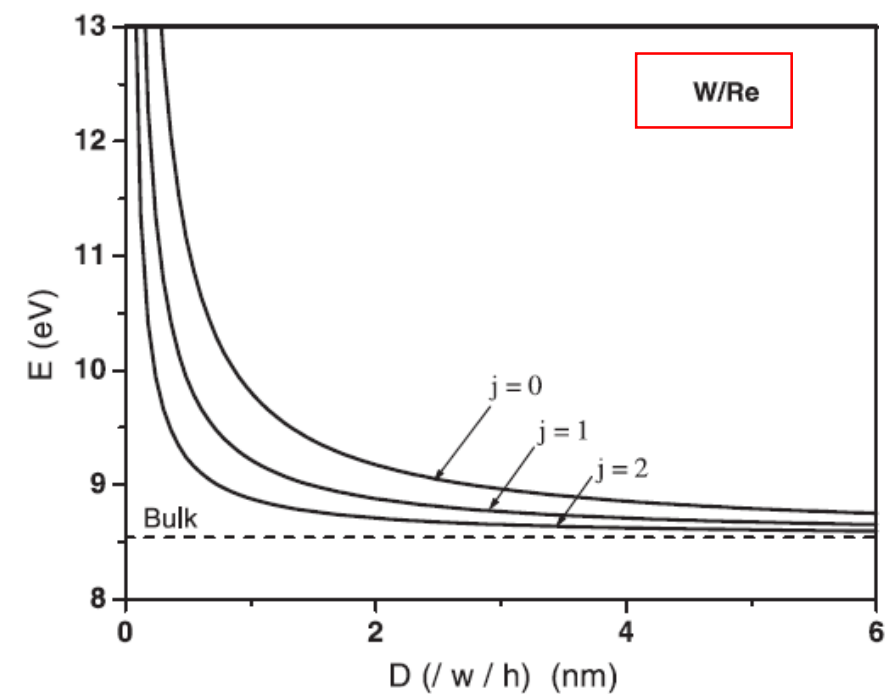
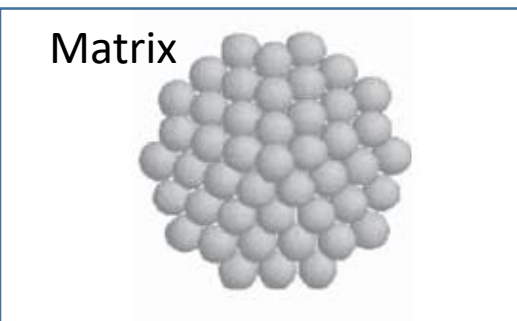


Figure 3. Cohesive energy of W nanocrystals embedded in a Re matrix. The solid lines are computed by equation (12), where $d_{100} = 0.31650$ nm [18], $E_b = 8.54$ eV [1] and $\alpha = 1.245$. The surface energies of W and Re are 2753 mJ m^{-2} and 3100 mJ m^{-2} [5], respectively, and $p = 0.126$.

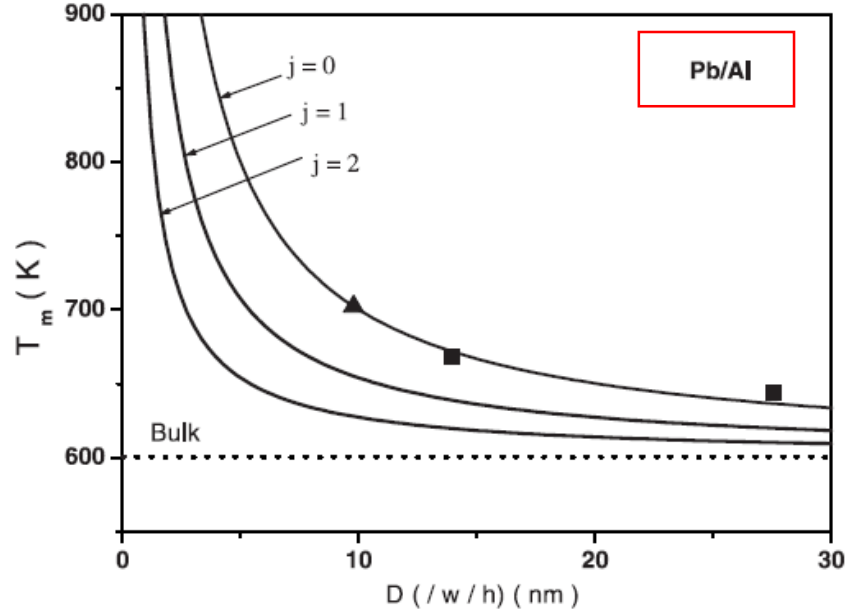


Figure 5. Melting temperature of Pb nanocrystals embedded in an Al matrix. The solid lines are theoretical results given by equation (14), where $d_{100} = 0.49502$ nm [18], $T_{mb} = 600.6$ K [21] and $\alpha = 1.245$. The surface energies of Pb and Al are 544 mJ m^{-2} and 1032 mJ m^{-2} [5], respectively, and $p = 0.897$. The symbols '▲' [13] and '■' [14] denote the corresponding experimental values.

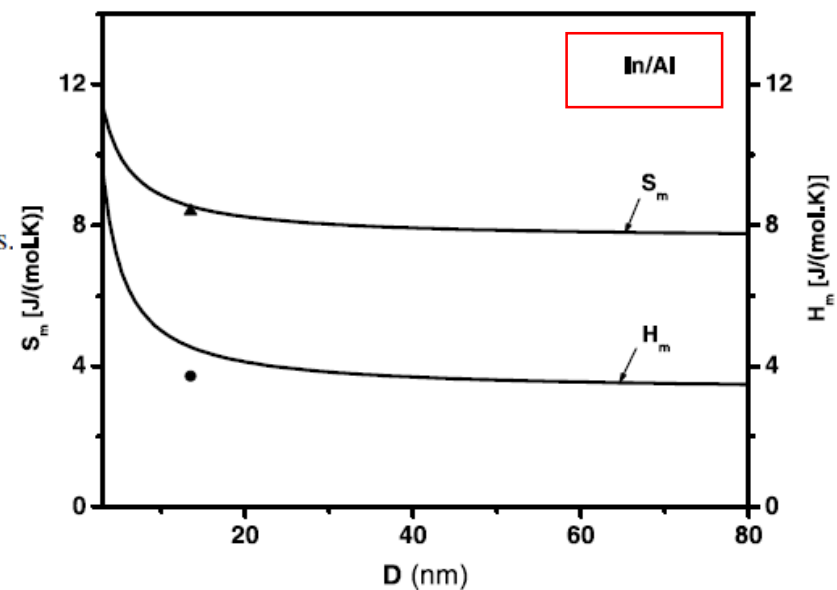


Figure 7. Melting entropy and melting enthalpy of In nanocrystals embedded in Al matrix. The solid lines denote the results calculated by equations (16) and (17), respectively, where $d_{100} = 0.45979$ nm [18], $H_{mb} = 3.27$ $\text{J mol}^{-1} \text{K}^{-1}$ [24], $S_{mb} = 7.60$ [24] and $\alpha = 1.245$. The surface energies of In and Al are 638 mJ m^{-2} and 1032 mJ m^{-2} [5], respectively, and $p = 0.617$. The symbols '▲' and '●' denote the corresponding experimental values [25].